Aust. J. Phys., 1995, **48**, 775–811

Systematics of the Electroweak Plasma at Finite Temperature II*

B. J. K. Smith, N. S. Witte and K. C. Hines

School of Physics, University of Melbourne,
Parkville, Vic. 3052, Australia.

Abstract

This paper extends the treatment of the polarisation tensor for the electroweak plasma to encompass all the preliminaries needed for a thorough study of its characteristics as they affect the early Universe. The detailed development of the one-loop polarisation tensor calculated in a previous paper includes the construction of the basis tensors in terms of which the polarisation tensor is most conveniently expressed. The polarisation response functions are obtained next and there follows a detailed discussion of the real and imaginary parts of the polarisation tensor. These are the essential tools for the subsequent study of the mode structure and dissipation properties of the electroweak plasma.

1. Introduction

The aim of the present work is to step back from the details of the early Universe and give a broad general discussion, within the framework of gauge field theory, of the behaviour of the particles involved using the polarisation tensor in the one-loop approximation. From the polarisation tensor, the thermodynamics and dispersion relations of the system can be obtained and the consequences of the appearance of an electroweak plasma in the early evolution of the Universe and any phase transitions that the electroweak plasma may undergo can then be evaluated. By using a systematic approach, the set of particles which make the main contribution to the phase transition can be obtained, which gives insight into the development required to extend the calculations.

The procedure used to obtain the polarisation tensor is given in Smith *et al.* (1995) hereinafter referred to as Paper I. There all contributions to the polarisation tensor of the electroweak plasma have been determined at the one-loop level.

The aim of the present paper (Paper II) is to continue with the analysis of the detailed mathematical properties of the polarisation tensor up to a stage at which meaningful investigation of the characteristics of the electroweak plasma can be undertaken.

The present paper begins by constructing the set of basis tensors in terms of which the polarisation tensor may most usefully be described. Following on

* Paper I, *Aust. J. Phys.* **48**, 739.

0004-9506/95/050775$15.00

from this the polarisation response functions are defined in equation (16) and then explicitly calculated using equations (55), (56) and (57) for the loop, tadpole and balloon diagrams respectively. These expressions are given in terms of the so-called Y and Z functions which turn out to be of great importance in the subsequent work.

In terms of these functions the real parts of the polarisation response functions are calculated next. The imaginary parts of the polarisation response functions are obtained from the study of electroweak plasma properties by extending the work of Tsytovich (1961) for the QED plasma to the electroweak plasma. The determination of the damping regions in Fourier space is dependent on the masses of the propagating particles and this leads to the definition of the imaginary parts of the polarisation response functions given in equation (135). From the real and imaginary parts of the polarisation response functions, the mode structure and dissipation properties of the electroweak plasma may be investigated, in principle.

The correspondence between each Feynman diagram and the equations and functions used to describe it is given in Table 5 of this paper.

2 Construction of the Polarisation Tensor

2.1 Basis Tensors

As we are interested in the first order self-energy shift, the incoming and outgoing particles are the same, so the polarisation tensor for a particular diagram will be symmetric. The most general symmetric second rank tensor that can be constructed for the isotropic system will be a linear combination of the invariants $q^\mu q_\mu$ and $q^\mu u_\mu$ and the symmetric tensors $g_{\mu\nu}$, $q_\mu q_\nu$, $u_\mu u_\nu$ and $q_\mu u_\nu + q_\nu u_\mu$, where u_μ is the 4-velocity of the frame co-moving with the plasma. It would be possible to specify the polarisation tensor in terms of this basis set; however, the more convenient choice is to use the set of orthogonal tensors $L_{\mu\nu}$, $T_{\mu\nu}$, $Q_{\mu\nu}$ and $C_{\mu\nu}$ given by

$$L_{\mu\nu} = \frac{(q\cdot u)^2}{q^2-(q\cdot u)^2}\left\{\frac{q_\mu q_\nu}{q^2} - \frac{q_\mu u_\nu + q_\nu u_\mu}{q\cdot u} + q^2\frac{u_\mu u_\nu}{(q\cdot u)^2}\right\}, \tag{1}$$

$$T_{\mu\nu} = g_{\mu\nu} + \frac{1}{q^2-(q\cdot u)^2}\left\{(q\cdot u)(q_\mu u_\nu + q_\nu u_\mu) - q^2(u_\mu u_\nu + \frac{q_\mu q_\nu}{q^2})\right\}, \tag{2}$$

$$Q_{\mu\nu} = \frac{q_\mu q_\nu}{q^2}, \tag{3}$$

$$C_{\mu\nu} = \frac{q_\mu u_\nu + q_\nu u_\mu}{2q\cdot u} - \frac{q_\mu q_\nu}{q^2}. \tag{4}$$

Here $T_{\mu\nu}$ and $L_{\mu\nu}$ are based on the tensors specified in Melrose (1982), while the other two are based on the tensors specified in Gross *et al.* (1981) recalculated to show explicitly the u_μ velocity.

A useful relationship between the tensors is

$$g_{\mu\nu} = L_{\mu\nu} + T_{\mu\nu} + Q_{\mu\nu}. \tag{5}$$

The calculations for the polarisation tensor are performed in the rest frame of the plasma, where $u = (1,0,0,0)$ and hence $q\cdot u = \omega$. The magnitude of the momentum 3-vector of the incoming particle is given by

$$\mathcal{Q} \equiv |\mathbf{q}|.$$

The tensors used are orthogonal with the following properties:

$$\begin{aligned}
T^{\mu\rho}L_{\rho\nu} &= 0, && (6)\\
T^{\mu\rho}Q_{\rho\nu} &= 0, && (7)\\
T^{\mu\rho}C_{\rho\nu} &= 0, && (8)\\
L^{\mu\rho}Q_{\rho\nu} &= 0, && (9)\\
L^{\mu\rho}C_{\rho\nu} &= 0, && (10)\\
Q^{\mu\rho}C_{\rho\nu} &= 0, && (11)\\
T^{\mu\rho}T_{\rho\nu} &= T^{\mu}{}_{\nu}, && (12)\\
L^{\mu\rho}L_{\rho\nu} &= L^{\mu}{}_{\nu}, && (13)\\
Q^{\mu\rho}Q_{\rho\nu} &= Q^{\mu}{}_{\nu}, && (14)\\
C^{\mu\rho}C_{\rho\nu} &= \frac{q^2-(q\cdot u)^2}{4q\cdot u^2}(L^{\mu}{}_{\nu}+Q^{\mu}{}_{\nu}). && (15)
\end{aligned}$$

2.2 Polarisation Response Functions

The polarisation tensor will be expressed using the set of tensors defined previously as

$$\Pi_{\mu\nu} = \pi^T T_{\mu\nu} + \pi^L L_{\mu\nu} + \pi^Q Q_{\mu\nu} + \pi^C C_{\mu\nu}. \tag{16}$$

Using the orthogonality of the basis tensors, the polarisation response functions used to describe the polarisation tensor are

$$\begin{aligned}
\pi^T &= \frac{\Pi_{\mu\nu}T^{\mu\nu}}{T_{\mu\nu}T^{\mu\nu}}, && (17)\\
\pi^L &= \frac{\Pi_{\mu\nu}L^{\mu\nu}}{L_{\mu\nu}L^{\mu\nu}}, && (18)\\
\pi^Q &= \frac{\Pi_{\mu\nu}Q^{\mu\nu}}{Q_{\mu\nu}Q^{\mu\nu}}, && (19)\\
\pi^C &= \frac{\Pi_{\mu\nu}C^{\mu\nu}}{C_{\mu\nu}C^{\mu\nu}}. && (20)
\end{aligned}$$

2.3 Other Tensors

Any other tensors can be given as a linear combination of the set described in Section 2.1. For example, those used by both Kapusta (1989) and Carrington (1992) are

$$\begin{aligned}
P_T^{\mu\nu} &= -T^{\mu\nu}, && (21)\\
P_L^{\mu\nu} &= -L^{\mu\nu}. && (22)
\end{aligned}$$

The set of tensors used by Gross *et al.* (1981) are

$$\begin{aligned}
A_{\mu\nu}^{\mathrm{GPY}} &= -T_{\mu\nu}, && (23)\\
B_{\mu\nu}^{\mathrm{GPY}} &= -L_{\mu\nu}, && (24)\\
C_{\mu\nu}^{\mathrm{GPY}} &= \sqrt{2}\frac{\omega}{Q}C_{\mu\nu}, && (25)\\
D_{\mu\nu}^{\mathrm{GPY}} &= Q_{\mu\nu}. && (26)
\end{aligned}$$

The set of tensors used by Melrose (1982) are

$$T^{\rm MEL}_{\mu\nu} = T_{\mu\nu}, \tag{27}$$

$$L^{\rm MEL}_{\mu\nu} = \frac{q^2}{\omega^2} L_{\mu\nu}. \tag{28}$$

In the rest frame, the ij components of these tensors are

$$\overleftrightarrow{\mathbf{T}}^{\rm MEL} = -\overleftrightarrow{\mathbf{I}} + \frac{\mathbf{q}\mathbf{q}}{Q^2}, \tag{29}$$

$$\overleftrightarrow{\mathbf{L}}^{\rm MEL} = -\frac{\mathbf{q}\mathbf{q}}{Q^2}, \tag{30}$$

hence these tensors can be considered as the covariant forms of the transverse and longitudinal 3-tensors respectively. The three dimensional tensors used by Tsytovich (1961) are the negative of the ij components of those used by Melrose (1982).

2.4 Propagators

2.4.1 Free Field Propagator

The propagator for a massive gauge boson for the R_ξ gauge and in the absence of external fields is given by

$$\mathcal{D}_{0\mu\nu} = \frac{1}{q^2 - m^2}\left[g_{\mu\nu} - \frac{q_\mu q_\nu}{m^2}\right] + \frac{q_\mu q_\nu}{m^2}\frac{1}{q^2 - \xi m^2}, \tag{31}$$

where q_μ is the wave 4-vector of the propagating particle and m is the mass of the gauge boson. This is a standard result of gauge field theory, e.g. Itzykson and Zuber (1980), Bailin and Love (1986) and others, which follows from the electroweak Lagrangian.

The inverse of a general propagator is defined by

$$\mathcal{D}^{\mu\alpha}\mathcal{D}^{-1}_{\alpha\nu} = g^\mu{}_\nu. \tag{32}$$

The inverse free field propagator is found by constructing a linear combination of the basis tensors, substituting this and the free field propagator in equation (32), performing the contraction and solving for the coefficients of the linear combination. This gives for the inverse free field propagator

$$\mathcal{D}_{0\mu\nu}^{-1} = (q^2 - m^2)g_{\mu\nu} + \frac{1-\xi}{\xi}q_\mu q_\nu. \tag{33}$$

2.4.2 Full Propagator

The Dyson equation states that the full propagator is related to the free field propagator and the polarisation tensor by

$$\mathcal{D}^{-1}_{\mu\nu} = \mathcal{D}^{-1}_{0\mu\nu} - \Pi_{\mu\nu}. \tag{34}$$

Using the form of the free field propagator given in equation (33) and the general form of the polarisation tensor given in equation (16), the Dyson equation gives for the inverse full propagator

$$
\begin{aligned}
\mathcal{D}^{-1}_{\mu\nu} &= (q^2 - m^2 - \pi^T)T_{\mu\nu} + (q^2 - m^2 - \pi^L)L_{\mu\nu} \\
&+ \left[\xi^{-1}q^2 - m^2 - \pi^Q\right] Q_{\mu\nu} + \pi^C C_{\mu\nu}.
\end{aligned} \tag{35}
$$

Here, the relationship between the basis tensors given in equation (5) has been used. The inverse full propagator is inverted using the same procedure as outlined in Section 2.4.1. This gives for the full propagator

$$
\begin{aligned}
\mathcal{D}_{\mu\nu} &= \frac{1}{q^2 - m^2 - \pi^T} T_{\mu\nu} + 4\omega^2(q^2 - \xi m^2 - \xi\pi^Q)\frac{1}{S}L_{\mu\nu} \\
&+ 4\xi\omega^2(q^2 - m^2 - \pi^L)\frac{1}{S}Q_{\mu\nu} + 4\xi\pi^C\omega^2\frac{1}{S}C_{\mu\nu},
\end{aligned} \tag{36}
$$

where S is defined to be

$$
S = \xi Q^2(\pi^C)^2 + 4\omega^2(q^2 - m^2 - \pi^L)(q^2 - \xi m^2 - \xi\pi^Q). \tag{37}
$$

As a check on this expression, for the case of no interactions, the polarisation response functions are all zero and equation (36) reduces to the free field propagator given in equation (31).

2.4.3 Ward's Identity

The full field propagator satisfies Ward's identity

$$
q_\mu q_\nu \mathcal{D}^{\mu\nu} = \xi. \tag{38}
$$

The full propagator given in equation (36) is used with Ward's identity. Also $q_\mu q_\nu$ is proportional to $Q_{\mu\nu}$, hence the contractions in equations (7), (9), (11) and (14) can be used. These show that only the term multiplying $Q_{\mu\nu}$ contributes when Ward's identity is applied. This gives

$$
(\pi^C)^2 = -4\frac{\omega^2}{Q^2}(q^2 - m^2 - \pi^L)(m^2 + \pi^Q), \tag{39}
$$

which can be rearranged to give

$$
\pi^Q = \frac{-4m^2\omega^2(q^2 - m^2 - \pi^L) - Q^2(\pi^C)^2}{4\omega^2(q^2 - m^2 - \pi^L)}. \tag{40}
$$

For the case where $m = 0$, equation (40) reduces to

$$
m = 0: \qquad \pi^Q = \frac{Q^2(\pi^C)^2}{4\omega^2(q^2 - \pi^L)}. \tag{41}
$$

Gross *et al.* (1981) considered Ward's identity applied to the case of QCD gluons. The basis tensors used there are given in equations (23) to (26) and when the difference in basis tensors is taken into account, equation (41) is equivalent to equation (4.6) of Gross *et al.* (1981).

2.4.4 *Infrared Limit*

The discrete variable ω_n arises from the periodic (anti-periodic) boundary conditions on the path integral and this leads to the definition of $\omega_n = i2n\pi T$ for bosons and ghosts and $\omega_n = i(2n+1)\pi T$ for fermions. For the analytically continued polarisation tensor, the infrared limit is defined by $\omega = 0, q \to 0$, as the limit $\omega \to 0$ is ill-defined.

The electric and magnetic masses at the one-loop level are obtained from the infrared limit of components of the polarisation tensor following Gross *et al.* (1981):

$$m_{\rm el}^2 = -\Pi^0{}_0(\omega = 0, \mathcal{Q} \to 0), \tag{42}$$

$$m_{\rm mag}^2 = \tfrac{1}{2}\Pi^i{}_i(\omega = 0, \mathcal{Q} \to 0). \tag{43}$$

The expressions for $\Pi^0{}_0$ and $\Pi^i{}_i$ are related to the polarisation tensor response functions by

$$\Pi^0{}_0 = -\frac{\mathcal{Q}^2}{q^2}\pi^L + \frac{\omega^2}{q^2}\pi^Q - \frac{\mathcal{Q}^2}{q^2}\pi^C, \tag{44}$$

$$\Pi^i{}_i = 2\pi^T + \frac{\omega^2}{q^2}\pi^L - \frac{\mathcal{Q}^2}{q^2}\pi^Q + \frac{\mathcal{Q}^2}{q^2}\pi^C. \tag{45}$$

2.5 Polarisation Response Functions

The polarisation tensor for a particular diagram is expressed in terms of the four polarisation response functions as stated in equation (16); namely

$$\Pi_{\mu\nu} = \pi^T T_{\mu\nu} + \pi^L L_{\mu\nu} + \pi^Q Q_{\mu\nu} + \pi^C C_{\mu\nu}. \tag{46}$$

For example, π^T is given by

$$\pi^T = \frac{\Pi_{\mu\nu}T^{\mu\nu}}{T_{\mu\nu}T^{\mu\nu}}, \tag{47}$$

and the expressions for π^L, π^Q and π^C follow in the usual way.

The polarisation tensors for the tadpole, loop and balloon diagrams can be expressed as an integral depending on one of the tensors $g_{\mu\nu}$, $p_\mu p_\nu$, $q_\mu q_\nu$ or $p_\mu q_\nu + q_\mu p_\nu$. From equation (47) each of these tensors is contracted with $T_{\mu\nu}$. Hence, the set of functions required to evaluate π^T is

$$Y_g^T[m_1, \mu_1] = \int \frac{d^3\mathbf{p}}{(2\pi)^3}\frac{F(E_\mathbf{p}(m_1), \mu_1)}{2E_\mathbf{p}(m_1)}\frac{g_{\mu\nu}T^{\mu\nu}}{T_{\mu\nu}T^{\mu\nu}}, \tag{48}$$

$$Y_{pp}^T[m_1, \mu_1] = \int \frac{d^3\mathbf{p}}{(2\pi)^3}\frac{F(E_\mathbf{p}(m_1), \mu_1)}{2E_\mathbf{p}(m_1)}\frac{p_\mu p_\nu T^{\mu\nu}}{T_{\mu\nu}T^{\mu\nu}}, \tag{49}$$

$$Y_{qq}^T[m_1, \mu_1] = \int \frac{d^3\mathbf{p}}{(2\pi)^3}\frac{F(E_\mathbf{p}(m_1), \mu_1)}{2E_\mathbf{p}(m_1)}\frac{q_\mu q_\nu T^{\mu\nu}}{T_{\mu\nu}T^{\mu\nu}}, \tag{50}$$

$$Z_g^T[m_1, m_2, \mu_1] = \int \frac{d^3\mathbf{p}}{(2\pi)^3}\frac{F(E_\mathbf{p}(m_1), \mu_1)}{2E_\mathbf{p}(m_1)}\frac{g_{\mu\nu}T^{\mu\nu}}{T_{\mu\nu}T^{\mu\nu}} \times \left[4(p\cdot q)^2 - (q^2 + m_1^2 - m_2^2)^2\right]^{-1}, \tag{51}$$

$$Z_{pp}^T[m_1, m_2, \mu_1] = \int \frac{d^3\mathbf{p}}{(2\pi)^3}\frac{F(E_\mathbf{p}(m_1), \mu_1)}{2E_\mathbf{p}(m_1)}\frac{p_\mu p_\nu T^{\mu\nu}}{T_{\mu\nu}T^{\mu\nu}}$$

$$\times \left[4(p{\cdot}q)^2 - (q^2+m_1^2-m_2^2)^2\right]^{-1}, \tag{52}$$

$$Z^T_{qq}[m_1,m_2,\mu_1] = \int \frac{d^3\mathbf{p}}{(2\pi)^3} \frac{F(E_{\mathbf{p}}(m_1),\mu_1)}{2E_{\mathbf{p}}(m_1)} \frac{q_\mu q_\nu T^{\mu\nu}}{T_{\mu\nu}T^{\mu\nu}} \times \left[4(p{\cdot}q)^2 - (q^2+m_1^2-m_2^2)^2\right]^{-1}, \tag{53}$$

$$Z^T_{pq}[m_1,m_2,\mu_1] = \int \frac{d^3\mathbf{p}}{(2\pi)^3} \frac{F(E_{\mathbf{p}}(m_1),\mu_1)}{2E_{\mathbf{p}}(m_1)} p{\cdot}q \frac{[p_\mu q_\nu + q_\mu p_\nu]T^{\mu\nu}}{T_{\mu\nu}T^{\mu\nu}} \times \left[4(p{\cdot}q)^2 - (q^2+m_1^2-m_2^2)^2\right]^{-1}. \tag{54}$$

The notation used here is that the Z functions have an integration over a denominator, while the Y functions do not. The subscript on the functions corresponds to the tensor (from the set of $g_{\mu\nu}$, $p_\mu p_\nu$, $q_\mu q_\nu$ or $p_\mu q_\nu + q_\mu p_\nu$) that is contracted with the basis tensor, and the basis tensor is given as the superscript.

The functions used to evaluate the π^L function are obtained by contracting the $L_{\mu\nu}$ tensor with each of $g_{\mu\nu}$, $p_\mu p_\nu$, $q_\mu q_\nu$ or $p_\mu q_\nu + q_\mu p_\nu$ and this would yield a set of functions similar to those shown above, with $T_{\mu\nu}$ replaced by $L_{\mu\nu}$ and hence the superscript T replaced by L. The same procedure is followed to give the functions used for the π^Q and π^C response functions.

The procedure used to calculate the polarisation tensor was given in Paper I and this can be represented as

$$\begin{matrix} \text{Vertices} \\ \text{Propagators} \end{matrix} \rightarrow X_{\mu\nu}(p) \rightarrow \begin{matrix} f_{\mu\nu}(p) \\ h_{\mu\nu}(p) \end{matrix} \rightarrow \begin{matrix} \mathcal{K}_i \\ \mathcal{M}_i \end{matrix} \rightarrow \Pi_{\mu\nu}(q).$$

The polarisation tensor is then expressed in terms of the polarisation response functions given above. As the constants $\mathcal{K}_i$ and $\mathcal{M}_i$ are independent of the integration variable, they can be taken outside the defined functions.

For example, the most general expression for the loop diagram polarisation tensor with gauge bosons in the external legs is taken from Paper I and the polarisation response function for this case is

$$\begin{aligned}
\pi^J = \tfrac{1}{2}\Big\{ & \tfrac14\mathcal{K}_2 Y^J_g[m_1,\mu_1] + \tfrac14\mathcal{K}_4 Y^J_{pp}[m_1,\mu_1] + \tfrac14\mathcal{K}_6 Y^J_{qq}[m_1,\mu_1] \\
&+ [\mathcal{K}_1 + \tfrac14\mathcal{K}_2(q^2+m_1^2-m_2^2)^2] Z^J_g[m_1,m_2,\mu_1] \\
&+ [\mathcal{K}_3 + \tfrac14\mathcal{K}_4(q^2+m_1^2-m_2^2)^2] Z^J_{pp}[m_1,m_2,\mu_1] \\
&+ [\mathcal{K}_5 + \tfrac14\mathcal{K}_6(q^2+m_1^2-m_2^2)^2] Z^J_{qq}[m_1,m_2,\mu_1] \\
&+ \mathcal{K}_7 Z^J_{pq}[m_1,m_2,\mu_1] \\
&+ \tfrac14\mathcal{M}_2 Y^J_g[m_2,\mu_2] + \tfrac14\mathcal{M}_4 Y^J_{pp}[m_2,\mu_2] + \tfrac14\mathcal{M}_6 Y^J_{qq}[m_2,\mu_2] \\
&+ [\mathcal{M}_1 + \tfrac14\mathcal{M}_2(q^2+m_2^2-m_1^2)^2] Z^J_g[m_2,m_1,\mu_2] \\
&+ [\mathcal{M}_3 + \tfrac14\mathcal{M}_4(q^2+m_2^2-m_1^2)^2] Z^J_{pp}[m_2,m_1,\mu_2] \\
&+ [\mathcal{M}_5 + \tfrac14\mathcal{M}_6(q^2+m_2^2-m_1^2)^2] Z^J_{qq}[m_2,m_1,\mu_2] \\
&+ \mathcal{M}_7 Z^J_{pq}[m_2,m_2,\mu_2]\Big\},
\end{aligned} \tag{55}$$

where J is one of $\{T, L, Q, C\}$. This gives a template for the results.

For example, the most general expression for the tadpole diagram polarisation tensor with gauge bosons in the external legs is taken from Paper I and the polarisation response function for this case is

$$\pi^T = \mathcal{K}_0 Y_g^T[m_1, \mu_1] + \mathcal{M}_0 Y_{pp}^T[m_1, \mu_1], \tag{56}$$

while the most general expression for the tadpole diagram polarisation tensor with gauge bosons in the external legs is taken from Paper I and the polarisation response function for this case is

$$\pi^T = \mathcal{K}_8 Y_g^T[m_1, \mu_1]. \tag{57}$$

The procedure given above has been implemented for the computer application Mathematica of Wolfram (1991) and the Mathematica package HIP of Hsieh and Yedudai (1992) to obtain the $\mathcal{K}_i$ and $\mathcal{M}_i$ constants for the most general types of Feynman diagrams. The $\mathcal{K}_i$ and $\mathcal{M}_i$ constants are not shown explicitly but rather have been combined with equations (56), (55) and (57) to give the polarisation response functions for diagrams with gauge bosons propagating in the external legs that are shown in Appendix B.

3 Real Part of the One-loop Polarisation Tensor

The one-loop polarisation tensor for a propagating particle is specified in terms of the tadpole, loop and balloon diagrams. These diagrams are constructed from the Y and Z functions and the polarisation tensor is analytically continued. The real part of the one-loop polarisation tensor is obtained by finding the real part of the Y and Z functions using the Plemelj rule. For the real part, the Plemelj rule simply specifies that the integration is a principal value integration. The Y functions have no singularity and hence no principal value integration is needed.

3.1 Polarisation Response Functions

The Y and Z functions are specified in equations (48) to (54). In the rest frame (defined in Section 2.1) we have

$$\begin{aligned} q_\mu T^{\mu\nu} &= 0, && (58)\\ p_\mu p_\nu T^{\mu\nu} &= \frac{(\mathbf{p}\cdot\mathbf{q})^2}{Q^2} - |\mathbf{p}|^2, && (59)\\ g_{\mu\nu} T^{\mu\nu} &= 2, && (60)\\ T_{\mu\nu} T^{\mu\nu} &= 2, && (61)\end{aligned}$$

$$\begin{aligned} q_\mu L^{\mu\nu} &= 0, && (62)\\ p_\mu p_\nu L^{\mu\nu} &= -\frac{1}{q^2}\left(E_{\mathbf{p}}(m_1)Q - \omega\frac{\mathbf{p}\cdot\mathbf{q}}{Q}\right)^2, && (63)\\ g_{\mu\nu} L^{\mu\nu} &= 1, && (64)\\ L_{\mu\nu} L^{\mu\nu} &= 1, && (65)\end{aligned}$$

$$q_\mu q_\nu Q^{\mu\nu} = q^2, \tag{66}$$

$$p_\mu p_\nu Q^{\mu\nu} = \frac{(p{\cdot}q)^2}{q^2}, \tag{67}$$
$$(p_\mu q_\nu + q_\mu p_\nu)Q^{\mu\nu} = 2p{\cdot}q, \tag{68}$$
$$g_{\mu\nu}Q^{\mu\nu} = 1, \tag{69}$$
$$Q_{\mu\nu}Q^{\mu\nu} = 1, \tag{70}$$

$$q_\mu q_\nu C^{\mu\nu} = 0, \tag{71}$$
$$p_\mu p_\nu C^{\mu\nu} = -\frac{(p{\cdot}q)^2}{q^2} + (p{\cdot}q)\frac{E_{\mathbf{p}}(m_1)}{\omega}, \tag{72}$$
$$(p_\mu q_\nu + q_\mu p_\nu)C^{\mu\nu} = q^2\left(-\frac{(p{\cdot}q)^2}{q^2} + (p{\cdot}q)\frac{E_{\mathbf{p}}(m_1)}{\omega}\right), \tag{73}$$
$$g_{\mu\nu}C^{\mu\nu} = 0, \tag{74}$$
$$C_{\mu\nu}C^{\mu\nu} = -\frac{Q^2}{2\omega^2}, \tag{75}$$

where $p{\cdot}q = E_{\mathbf{p}}(m_1)\omega - \mathbf{p}\cdot\mathbf{q}$.

This has been left in the general form as cylindrical coordinates are used later. Here, spherical co-ordinates are used, with the z axis chosen to be along $\mathbf{q}$, hence $\cos\theta$ is the angle between $\mathbf{p}$ and $\mathbf{q}$. The notation is

$$\mathcal{P} \equiv |\mathbf{p}|. \tag{76}$$

3.1.1 Y^T Functions

Using equation (58) the Y^T_{qq} function is identically zero. For the other Y^T functions the only occurrence of θ is due to $p_\mu p_\nu T^{\mu\nu}$, and hence the θ integration is simple and along with the ϕ integration can be performed immediately. The integrals are expressed in terms of dimensionless parameters

$$Y^T_g[m_1, \mu_1] = \frac{1}{4\pi^2}T^2\Gamma[3]H_3\left(\frac{m_1}{T}, \frac{\mu_1}{m_1}\right), \tag{77}$$
$$Y^T_{pp}[m_1, \mu_1] = -\frac{1}{12\pi^2}T^4\Gamma[5]H_5\left(\frac{m_1}{T}, \frac{\mu_1}{m_1}\right), \tag{78}$$

where the H_l functions were defined by Haber and Weldon (1982*a,b*) and are given by

$$H_l(y,r) = \frac{1}{\Gamma(l)}\int_0^\infty \frac{x^{l-1}dx}{(x^2+y^2)^{1/2}}\left(\frac{1}{\exp\left[(x^2+y^2)^{1/2} - yr\right] - 1} + r \to -r\right). \tag{79}$$

Here, and generally, the $r \to -r$ notation means that the second term in the large parentheses is given by the first term under this substitution. The Bose–Einstein distribution function is used as it has been assumed that bosons are propagating in the loop. When fermions are propagating in the loop, the Fermi–Dirac distribution function will be used in the expression for H_l.

3.1.2 Z^T Functions

Using equation (58) the Z^T_{qq} and Z^T_{pq} functions are identically zero. For the other Z^T functions the ϕ integration can be performed immediately; however, the θ integration is more difficult due to the $p\cdot q$ term in the denominator. For bosons propagating in the loop

$$\begin{aligned} \mathrm{Re}\, Z^T_g[m_1, m_2, \mu_1] &= \\ \frac{1}{8\pi^2}\int_0^\infty \frac{\mathcal{P}^2 d\mathcal{P}}{(\mathcal{P}^2+m_1^2)^{\frac{1}{2}}} & \left[\frac{1}{\exp\left[\frac{(\mathcal{P}^2+m_1^2)^{\frac{1}{2}}-\mu_1}{T}\right]-1} + \mu_1 \to -\mu_1\right] \\ \times \int_{-1}^{+1} d(\cos\theta) & \frac{1}{4\left[(\mathcal{P}^2+m_1^2)^{\frac{1}{2}}\omega - \mathcal{P}\mathcal{Q}\cos\theta\right]^2 - (q^2+m_1^2-m_2^2)^2}, \end{aligned} \tag{80}$$

$$\begin{aligned} \mathrm{Re}\, Z^T_{pp}[m_1, m_2, \mu_1] &= \\ \frac{1}{16\pi^2}\int_0^\infty \frac{\mathcal{P}^4 d\mathcal{P}}{(\mathcal{P}^2+m_1^2)^{\frac{1}{2}}} & \left[\frac{1}{\exp\left[\frac{(\mathcal{P}^2+m_1^2)^{\frac{1}{2}}-\mu_1}{T}\right]-1} + \mu_1 \to -\mu_1\right] \\ \times \int_{-1}^{+1} d(\cos\theta) & \frac{\cos^2\theta - 1}{4\left[(\mathcal{P}^2+m_1^2)^{\frac{1}{2}}\omega - \mathcal{P}\mathcal{Q}\cos\theta\right]^2 - (q^2+m_1^2-m_2^2)^2}. \end{aligned} \tag{81}$$

The general form of the integrals over θ are

$$\int_{-1}^{+1} d(\cos\theta)\frac{1}{4(a-b\cos\theta)^2-c^2} = \frac{1}{4bc}\ln\left|\frac{4a^2-(2b-c)^2}{4a^2-(2b+c)^2}\right|, \tag{82}$$

$$\begin{aligned} \int_{-1}^{+1} d(\cos\theta)\frac{\cos\theta}{4(a-b\cos\theta)^2-c^2} &= \frac{1}{8b^2}\ln\left|\frac{4(a-b)^2-c^2}{4(a+b)^2-c^2}\right| \\ &+ \frac{a}{4b^2c}\ln\left|\frac{4a^2-(2b-c)^2}{4a^2-(2b+c)^2}\right|, \end{aligned} \tag{83}$$

$$\begin{aligned} \int_{-1}^{+1} d(\cos\theta)\frac{\cos^2\theta}{4(a-b\cos\theta)^2-c^2} &= \frac{1}{2b^2} + \frac{a}{4b^3}\ln\left|\frac{4(a-b)^2-c^2}{4(a+b)^2-c^2}\right| \\ &+ \frac{4a^2+c^2}{16b^3c}\ln\left|\frac{4a^2-(2b-c)^2}{4a^2-(2b+c)^2}\right|, \end{aligned} \tag{84}$$

where these results have been obtained by straightforward integration.

Hence the expressions for the real part of the Z^T functions are

$$
\begin{aligned}
\mathrm{Re}\, Z_g^T[m_1, m_2, \mu_1] &= \\
&\frac{1}{32\pi^2 \mathcal{Q}} \frac{1}{(q^2 + m_1^2 - m_2^2)} \\
&\times \int_0^\infty \frac{\mathcal{P} d\mathcal{P}}{(\mathcal{P}^2 + m_1^2)^{\frac{1}{2}}} \left[\frac{1}{\exp\left[\frac{(\mathcal{P}^2+m_1^2)^{\frac{1}{2}} - \mu_1}{T}\right] - 1} + \mu_1 \to -\mu_1 \right] \ln \Lambda_0, \qquad (85)
\end{aligned}
$$

$$
\begin{aligned}
\mathrm{Re}\, Z_{pp}^T[m_1, m_2, \mu_1] &= \\
&\frac{1}{32\pi^2 \mathcal{Q}^2} \int_0^\infty \frac{\mathcal{P}^2 d\mathcal{P}}{(\mathcal{P}^2 + m_1^2)^{\frac{1}{2}}} \left[\frac{1}{\exp\left[\frac{(\mathcal{P}^2+m_1^2)^{\frac{1}{2}} - \mu_1}{T}\right] - 1} + \mu_1 \to -\mu_1 \right] \\
&\times \left\{ 1 + \frac{\omega}{2\mathcal{Q}} \frac{(\mathcal{P}^2 + m_1^2)^{\frac{1}{2}}}{p} \ln \Lambda_1 \right. \\
&\left. + \left[\mathcal{P} \frac{q^2}{2\mathcal{Q}(q^2 + m_1^2 - m_2^2)} + \frac{1}{\mathcal{P}} \frac{4m_1^2\omega^2 + (q^2 + m_1^2 - m_2^2)^2}{8\mathcal{Q}(q^2 + m_1^2 - m_2^2)} \right] \ln \Lambda_0 \right\},
\end{aligned}
$$
(86)

where

$$
\Lambda_0 = \left| \frac{4(\mathcal{P}^2 + m_1^2)\omega^2 - \left[2\mathcal{P}\mathcal{Q} - (q^2 + m_1^2 - m_2^2)\right]^2}{4(\mathcal{P}^2 + m_1^2)\omega^2 - \left[2\mathcal{P}\mathcal{Q} + (q^2 + m_1^2 - m_2^2)\right]^2} \right|, \qquad (87)
$$

$$
\Lambda_1 = \left| \frac{4\left[(\mathcal{P}^2 + m_1^2)^{\frac{1}{2}}\omega - \mathcal{P}\mathcal{Q}\right]^2 - (q^2 + m_1^2 - m_2^2)^2}{4\left[(\mathcal{P}^2 + m_1^2)^{\frac{1}{2}}\omega + \mathcal{P}\mathcal{Q}\right]^2 - (q^2 + m_1^2 - m_2^2)^2} \right|. \qquad (88)
$$

For fermions propagating in the loop, the Fermi–Dirac distribution function will be used.

3.1.3 Y^L and Z^L Functions

The Y^L and Z^L functions are developed in a similar manner to the Y^T and Z^T. The Y^L functions for bosons propagating in the loop are

$$
Y_g^L[m_1, \mu_1] = Y_g^T[m_1, \mu_1], \qquad (89)
$$

$$
\begin{aligned}
Y_{pp}^L[m_1, \mu_1] &= -\frac{1}{4\pi^2 q^2} \left[\left(\mathcal{Q}^2 + \frac{\omega^2}{3} \right) T^4 \Gamma[5] H_5 \left(\frac{m_1}{T}, \frac{\mu_1}{m_1} \right) \right. \\
&\left. + m_1^2 \mathcal{Q}^2 T^2 \Gamma[3] H_3 \left(\frac{m_1}{T}, \frac{\mu_1}{m_1} \right) \right]. \qquad (90)
\end{aligned}
$$

The Z^L functions for bosons propagating in the loop are

$$Z_g^L[m_1, m_2, \mu_1] = Z_g^T[m_1, m_2, \mu_1], \tag{91}$$

$$\begin{aligned}
\text{Re } Z_{pp}^L[m_1, m_2, \mu_1] =& \\
& -\frac{1}{16\pi^2 q^2 Q^2}\int_0^\infty \frac{\mathcal{P}^2 d\mathcal{P}}{(\mathcal{P}^2+m_1^2)^{\frac{1}{2}}}\left[\frac{1}{\exp\left[\frac{(\mathcal{P}^2+m_1^2)^{\frac{1}{2}}-\mu_1}{T}\right]-1}+\mu_1 \to -\mu_1\right] \\
& \times\left\{\omega^2 + \frac{\omega q^2}{2Q}\frac{(\mathcal{P}^2+m_1^2)^{\frac{1}{2}}}{\mathcal{P}}\ln\Lambda_1\right. \\
& \left. + \left[\mathcal{P}\frac{q^4}{2Q(q^2+m_1^2-m_2^2)}+\frac{1}{\mathcal{P}}\frac{4m_1^2q^4+\omega^2(q^2+m_1^2-m_2^2)^2}{8Q(q^2+m_1^2-m_2^2)}\right]\ln\Lambda_0\right\}.
\end{aligned} \tag{92}$$

For fermions propagating in the loop, the Fermi–Dirac distribution function will be used.

3.1.4 Y^Q and Z^Q Functions

The Y^Q and Z^Q functions are developed in a similar manner to the Y^T and Z^T. The Y^Q functions for bosons propagating in the loop are

$$Y_g^Q[m_1, \mu_1] = Y_g^T[m_1, \mu_1], \tag{93}$$

$$\begin{aligned}
Y_{pp}^Q[m_1, \mu_1] =& \frac{1}{4\pi^2 q^2}\left[\left(\omega^2+\frac{Q^2}{3}\right)T^4\Gamma[5]H_5\left(\frac{m_1}{T},\frac{\mu_1}{m_1}\right)\right. \\
& \left. + m_1^2\omega^2T^2\Gamma[3]H_3\left(\frac{m_1}{T},\frac{\mu_1}{m_1}\right)\right],
\end{aligned} \tag{94}$$

$$Y_{qq}^Q[m_1, \mu_1] = q^2 Y_g^T[m_1, \mu_1]. \tag{95}$$

The Z^Q functions for bosons propagating in the loop are

$$Z_g^Q[m_1, m_2, \mu_1] = Z_g^T[m_1, m_2, \mu_1], \tag{96}$$

$$Z_{pp}^Q[m_1, m_2, \mu_1] = \frac{1}{4q^2}\left\{Y_g^T[m_1, \mu_1] + (q^2+m_1^2-m_2^2)^2 Z_g^T[m_1, m_2, \mu_1]\right\}, \tag{97}$$

$$Z_{pq}^Q[m_1, m_2, \mu_1] = \tfrac{1}{2}\left\{Y_g^T[m_1, \mu_1] + (q^2+m_1^2-m_2^2)^2 Z_g^T[m_1, m_2, \mu_1]\right\}, \tag{98}$$

$$Z_{qq}^Q[m_1, m_2, \mu_1] = q^2 Z_g^T[m_1, m_2, \mu_1]. \tag{99}$$

For fermions propagating in the loop, the Fermi–Dirac distribution function will be used.

3.1.5 Y^C and Z^C Functions

Using equations (74) and (71) the Y_g^C, Y_{qq}^C, Z_g^C and Z_{qq}^C functions are identically zero. The other Y^C and Z^C functions are developed in a similar manner to the

Y^T and Z^T functions. The Y^C_{pp} function for bosons propagating in the loop are

$$Y^C_{pp}[m_1,\mu_1] \;=\; \frac{1}{2\pi^2}\frac{\omega^2}{q^2}\left[\frac{4}{3}T^4\Gamma[5]H_5\left(\frac{m_1}{T},\frac{\mu_1}{m_1}\right) + m_1^2T^2\Gamma[3]H_3\left(\frac{m_1}{T},\frac{\mu_1}{m_1}\right)\right]. \tag{100}$$

The Z^C functions for bosons propagating in the loop are

$$\begin{aligned} \mathrm{Re}\, Z^C_{pp}[m_1,m_2,\mu_1] \;&=\; \\ &\frac{1}{8\pi^2}\frac{\omega^2}{Q^2}\int_0^\infty \frac{\mathcal{P}^2 d\mathcal{P}}{(\mathcal{P}^2+m_1^2)^{\frac{1}{2}}}\left[\frac{1}{\exp\left[\frac{(\mathcal{P}^2+m_1^2)^{\frac{1}{2}}-\mu_1}{T}\right]-1} + \mu_1 \to -\mu_1\right] \\ &\times\left\{\frac{1}{q^2} + \frac{1}{4\omega Q}\frac{(\mathcal{P}^2+m_1^2)^{\frac{1}{2}}}{\mathcal{P}}\ln\Lambda_1 + \frac{1}{\mathcal{P}}\frac{(q^2+m_1^2-m_2^2)^2}{8Qq^2}\ln\Lambda_0\right\}, \end{aligned} \tag{101}$$

$$Z^C_{pq}[m_1,m_2,\mu_1] \;=\; q^2 Z^C_{pp}[m_1,m_2,\mu_1]. \tag{102}$$

For fermions propagating in the loop, the Fermi–Dirac distribution function will be used.

4 Imaginary Parts

The one-loop polarisation tensor for a propagating particle is specified in terms of the tadpole, loop and balloon diagrams. These diagrams are constructed from the Y and Z functions. The imaginary part of the one-loop polarisation tensor is obtained by finding the imaginary part of the Y and Z functions.

4.1 Resonant Denominators

The imaginary parts of the Y and Z functions are obtained by using the Plemelj rule

$$\frac{1}{x \pm i\alpha} = P\frac{1}{x} \mp i\pi\delta(x). \tag{103}$$

The term on the left-hand side is a resonant denominator. The Y functions have no denominator of this form and hence have zero imaginary part.

The resonant denominator common to the Z functions is expressed in the compact form $4(p{\cdot}q)^2-(q^2+m_1^2-m_2^2)^2$. This can be expanded out, under $p^0 = E_{\mathbf{p}}(m_1)$, using

$$(E_{\mathbf{p}}(m_1) \pm q^0)^2 - E^2_{\mathbf{p}\pm\mathbf{q}}(m_2) = \pm 2(p{\cdot}q) + (q^2+m_1^2-m_2^2). \tag{104}$$

As an example, consider a general Z function $Z^J_{pp}[m_1,m_2,\mu_1]$, where J is one of $\{T,L,Q,C\}$,

$$\begin{aligned} &Z^J_{pp}[m_1,m_2,\mu_1] \\ &= \frac{-1}{2(q^2+m_1^2-m_2^2)}\int\frac{d^3p}{(2\pi)^3}\frac{F(E_{\mathbf{p}}(m_1),\mu_1)}{2E_{\mathbf{p}}(m_1)}\frac{p_\mu p_\nu J^{\mu\nu}}{J^{\mu\nu}J_{\mu\nu}} \end{aligned}$$

$$\times\left\{\frac{1}{2E_{\mathbf{p-q}}(m_2)}\left[\frac{1}{E_{\mathbf{p}}(m_1)-\omega-E_{\mathbf{p-q}}(m_2)}-\frac{1}{E_{\mathbf{p}}(m_1)-\omega+E_{\mathbf{p-q}}(m_2)}\right]\right.$$
$$\left.+\frac{1}{2E_{\mathbf{p+q}}(m_2)}\left[\frac{1}{E_{\mathbf{p}}(m_1)+\omega-E_{\mathbf{p+q}}(m_2)}-\frac{1}{E_{\mathbf{p}}(m_1)+\omega+E_{\mathbf{p+q}}(m_2)}\right]\right\}. \tag{105}$$

Here ω is understood as $\omega=\omega+i\varepsilon$ with $\varepsilon \to 0^+$.

A cylindrical co-ordinate system is used where the z axis is taken along the direction of the wave vector $\mathbf{q}$. The notation is

$$\mathbf{p} = (\mathcal{P}_z, \mathcal{P}_\perp, \phi), \tag{106}$$
$$\mathbf{q} = (\mathcal{Q}, 0, 0), \tag{107}$$

and in this co-ordinate system

$$\frac{p_\mu p_\nu J^{\mu\nu}}{J^{\mu\nu}J_{\mu\nu}} \equiv Z^J_{pp}[\mathcal{P}_z, \mathcal{P}_\perp]. \tag{108}$$

The Plemelj rule is applied and the imaginary part of the $Z^J_{pp}[m_1, m_2, \mu_1]$ function is

$$\begin{aligned}
\mathrm{Im}\, Z^J_{pp}&[m_1, m_2, \mu_1] \\
= &\frac{-1}{8(q^2+m_1^2-m_2^2)}\int\frac{d^3p}{(2\pi)^3}F(E_{\mathbf{p}}(m_1),\mu_1)Z^J_{pp}[\mathcal{P}_z,\mathcal{P}_\perp] \\
&\times\left\{\frac{1}{E_{\mathbf{p}}(m_1)E_{\mathbf{p-q}}(m_2)}\left[\pi\delta\left(E_{\mathbf{p}}(m_1)-\omega-E_{\mathbf{p-q}}(m_2)\right)\right.\right. \\
&\qquad\left.-\pi\delta\left(E_{\mathbf{p}}(m_1)-\omega+E_{\mathbf{p-q}}(m_2)\right)\right] \\
&+\frac{1}{E_{\mathbf{p}}(m_1)E_{\mathbf{p+q}}(m_2)}\left[-\pi\delta\left(E_{\mathbf{p}}(m_1)+\omega-E_{\mathbf{p+q}}(m_2)\right)\right. \\
&\qquad\left.\left.+\pi\delta\left(E_{\mathbf{p}}(m_1)+\omega+E_{\mathbf{p+q}}(m_2)\right)\right]\right\}.
\end{aligned} \tag{109}$$

4.2 Absorption Processes

The delta functions in equation (109) express the conservation of energy and momentum for the physical processes occurring in the plasma. The energy conservation relations for the physical processes are Tsytovich (1961)

$$\text{Cerenkov emission:}\quad E_{\mathbf{p}}(m_1)-\omega-E_{\mathbf{p-q}}(m_2) = 0, \tag{110}$$
$$\text{Pair production:}\quad E_{\mathbf{p}}(m_1)-\omega+E_{\mathbf{p-q}}(m_2) = 0, \tag{111}$$
$$\text{Cerenkov absorption:}\quad E_{\mathbf{p}}(m_1)+\omega-E_{\mathbf{p+q}}(m_2) = 0, \tag{112}$$
$$\text{Pair absorption:}\quad E_{\mathbf{p}}(m_1)+\omega+E_{\mathbf{p+q}}(m_2) = 0. \tag{113}$$

It is conventional to describe disturbances in the plasma in terms of positive frequencies. The reality condition implies that positive and negative frequencies in the polarisation tensor specify the same information; hence, following Melrose and McPhedran (1993), we can specialise to the region of positive ω and positive $\mathcal{Q}$. In this region the pair absorption process has no solutions, as the energies of the particles must be positive. The pair production process corresponds to the energy of the propagating particle being used to create two particles, momentum being absorbed by the medium. The Cerenkov processes correspond to part of the energy of the propagating particle being absorbed by the particles in the medium, the two possible processes corresponding to the way in which the energy can be shared.

The energy conservation equations for the processes occurring in the plasma are all solved by squaring both sides of the equation, re-arranging and squaring both sides again. This leads to the set of solutions for $\mathcal{P}_z$ (in terms of the masses, ω, $\mathcal{Q}$ and $\mathcal{P}_\perp$)

$$\mathcal{P}_z^A = -\tfrac{1}{2}\mathcal{Q}\left(1+\frac{m_1^2-m_2^2}{\omega^2-\mathcal{Q}^2}\right)+\frac{\omega}{\mathcal{Q}}\chi, \tag{114}$$

$$\mathcal{P}_z^B = -\tfrac{1}{2}\mathcal{Q}\left(1+\frac{m_1^2-m_2^2}{\omega^2-\mathcal{Q}^2}\right)-\frac{\omega}{\mathcal{Q}}\chi, \tag{115}$$

$$\mathcal{P}_z^C = +\tfrac{1}{2}\mathcal{Q}\left(1+\frac{m_1^2-m_2^2}{\omega^2-\mathcal{Q}^2}\right)+\frac{\omega}{\mathcal{Q}}\chi, \tag{116}$$

$$\mathcal{P}_z^D = +\tfrac{1}{2}\mathcal{Q}\left(1+\frac{m_1^2-m_2^2}{\omega^2-\mathcal{Q}^2}\right)-\frac{\omega}{\mathcal{Q}}\chi, \tag{117}$$

where

$$\chi \equiv \sqrt{\tfrac{1}{4}\mathcal{Q}^2\left(1+\frac{m_1^2-m_2^2}{\omega^2-\mathcal{Q}^2}\right)^2+\frac{\mathcal{P}_\perp^2+m_1^2}{1-\omega^2/\mathcal{Q}^2}}. \tag{118}$$

The expressions $\mathcal{P}_z^A$ and $\mathcal{P}_z^B$ relate to the Cerenkov process given by equation (112), while the expressions $\mathcal{P}_z^C$ and $\mathcal{P}_z^D$ relate to the Cerenkov process given by equation (110) and the pair production process given by equation (111), respectively. All of the expressions $\mathcal{P}_z^i$ are defined under the condition that $\chi^2 > 0$, and hence these absorption processes have solutions only in a particular region of the $(\omega, \mathcal{Q})$ plane. Equation (118) can be re-expressed as

$$\chi = \sqrt{\frac{\mathcal{Q}^2}{4(\omega^2-\mathcal{Q}^2)^2}(\omega^2-\mathcal{Q}^2-z_1^2)(\omega^2-\mathcal{Q}^2-z_2^2)}, \tag{119}$$

where

$$z_1 = \sqrt{\mathcal{P}_\perp^2+m_1^2}+\sqrt{\mathcal{P}_\perp^2+m_2^2}, \tag{120}$$

$$z_2 = \sqrt{\mathcal{P}_\perp^2+m_1^2}-\sqrt{\mathcal{P}_\perp^2+m_2^2}. \tag{121}$$

In the region of the $(\omega, \mathcal{Q})$ plane where $\chi^2 < 0$, equations (110) to (113) have no solutions and hence there will be no damping as the particle propagates through the medium. From equation (119) this region of the $(\omega, \mathcal{Q})$ plane is given by

$$z_1 > \omega^2 - \mathcal{Q}^2 > z_2. \tag{122}$$

This condition depends on $\mathcal{P}_\perp$, an integration variable which ranges from zero to infinity. The region given in equation (122) changes with $\mathcal{P}_\perp$ because z_1 increases as $\mathcal{P}_\perp$ increases, while z_2 decreases as $\mathcal{P}_\perp$ increases. Hence the region of the $(\omega, \mathcal{Q})$ plane where $\chi^2 < 0$ for all values of $\mathcal{P}_\perp$ is obtained by setting $\mathcal{P}_\perp = 0$ in equation (122). This gives

$$\text{Non-damping region:} \qquad \sqrt{\mathcal{Q}^2 + (m_1 + m_2)^2} \;>\; \omega \;>\; \sqrt{\mathcal{Q}^2 + (m_1 - m_2)^2}.$$

Hence, in the $(\omega, \mathcal{Q})$ plane, the curve $\omega = \sqrt{\mathcal{Q}^2 + (m_1 + m_2)^2}$ and the curve $\omega = \sqrt{\mathcal{Q}^2 + (m_1 - m_2)^2}$ define the region where $\chi^2 < 0$ and hence the region where no absorption processes are possible. This region is shaded in Fig. 1. For $m_1 < m_2$ the dashed line above $\omega = \mathcal{Q}$ is the solution to $\frac{m_1^2 - m_2^2}{\omega^2 - \mathcal{Q}^2} = -1$ and the dashed line below $\omega = \mathcal{Q}$ is the solution to $\frac{m_1^2 - m_2^2}{\omega^2 - \mathcal{Q}^2} = +1$. For $m_1 > m_2$ this identification is reversed. The regions 1, 2 and 3 relate to solution regions given later.

4.3 Energy Solutions

The energy corresponding to a particular expression for $\mathcal{P}_z$ is found by substituting this value of $\mathcal{P}_z$ back into the energy equations. For $\mathcal{P}_z^A$ this gives

$$E^A_{\mathbf{p}}(m_1) = \sqrt{\mathcal{P}_z^{A\,2} + \mathcal{P}_\perp^2 + m_1^2} = \left|\tfrac{1}{2}\omega\left(1 + \frac{m_1^2 - m_2^2}{\omega^2 - \mathcal{Q}^2}\right) - \chi\right|, \tag{123}$$

$$E^A_{\mathbf{p+q}}(m_2) = \sqrt{(\mathcal{P}_z^A + \mathcal{Q})^2 + \mathcal{P}_\perp^2 + m_1^2} = \left|\tfrac{1}{2}\omega\left(1 - \frac{m_1^2 - m_2^2}{\omega^2 - \mathcal{Q}^2}\right) + \chi\right|. \tag{124}$$

The expressions for both $E^A_{\mathbf{p}}(m_1)$ and $E^A_{\mathbf{p+q}}(m_2)$ involve a modulus sign so we need to examine the relative sign and magnitudes of the terms on the right-hand sides. The sign of $\frac{m_1^2 - m_2^2}{\omega^2 - \mathcal{Q}^2}$ depends on the region of the $(\omega, \mathcal{Q})$ plane and also depends on whether $m_1 > m_2$ or $m_1 < m_2$. Hence we may have different expressions for $E^A_{\mathbf{p}}(m_1)$ and $E^A_{\mathbf{p+q}}(m_2)$ in a particular region for each case. Table 1 gives for each region shown in Fig. 1 the sign of $\frac{m_1^2 - m_2^2}{\omega^2 - \mathcal{Q}^2}$ and the expression for $E^A_{\mathbf{p}}(m_1)$ and $E^A_{\mathbf{p+q}}(m_2)$ given by equations (123) and (124) respectively, for $m_1 < m_2$.

The absorption processes detailed in Section 4.2 can now be examined. The expressions for $E^A_{\mathbf{p}}(m_1)$ and $E^A_{\mathbf{p+q}}(m_2)$ given in Table 1 show that the Cerenkov process described by equation (112), viz. $E_{\mathbf{p}}(m_1) + \omega - E_{\mathbf{p+q}}(m_2) = 0$, is solved by $\mathcal{P}_z = \mathcal{P}_z^A$ for $m_1 < m_2$ in Regions 2 and 3 only.

The same procedure is followed for the case where $m_1 > m_2$ and the results are given in Table 2. Examining the expressions given for $E^A_{\mathbf{p}}(m_1)$ and $E^A_{\mathbf{p+q}}(m_2)$ shows that the Cerenkov process given by equation (112), viz. $E_{\mathbf{p}}(m_1) + \omega - E_{\mathbf{p+q}}(m_2) = 0$, is solved by $\mathcal{P}_z = \mathcal{P}_z^A$ for $m_1 > m_2$ in Region 3 only.

The same procedure is followed for all the $\mathcal{P}_z^i$ expressions. The results are given in Tables 3 and 4 and show the region of the $(\omega, \mathcal{Q})$ plane where the $\mathcal{P}_z$ expression is applicable for the process considered. This work indicates that the pair production process specified by equation (111) has solutions only for ω and $\mathcal{Q}$ in Region 1 and these solutions are given by $\mathcal{P}_z^C$ and $\mathcal{P}_z^D$. For ω and $\mathcal{Q}$ in Region 3

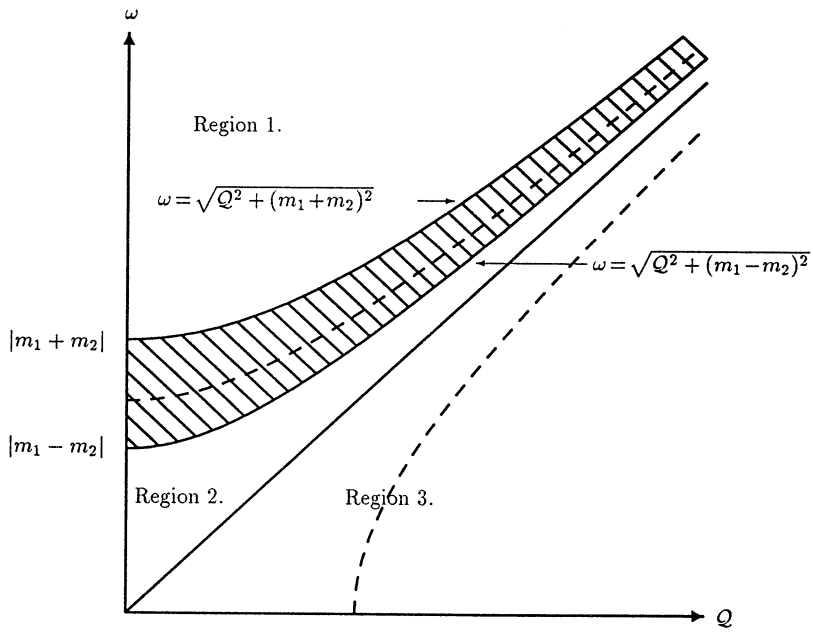

Figure 1. Non-damping region (shaded) for $m_1 < m_2$.

Region	$\frac{m_1^2-m_2^2}{\omega^2-Q^2}$	$E^A_{\mathbf{p}}(m_1)$	$E^A_{\mathbf{p}+\mathbf{q}}(m_2)$
1	$-1 < ... < 0$	$\frac{1}{2}\omega\left(1+\frac{m_1^2-m_2^2}{\omega^2-Q^2}\right)-\chi$	$\frac{1}{2}\omega\left(1-\frac{m_1^2-m_2^2}{\omega^2-Q^2}\right)+\chi$
2	$... < -1$	$\chi-\frac{1}{2}\omega\left(1+\frac{m_1^2-m_2^2}{\omega^2-Q^2}\right)$	$\frac{1}{2}\omega\left(1-\frac{m_1^2-m_2^2}{\omega^2-Q^2}\right)+\chi$
3	$... > 0$	$\chi-\frac{1}{2}\omega\left(1+\frac{m_1^2-m_2^2}{\omega^2-Q^2}\right)$	$\frac{1}{2}\omega\left(1-\frac{m_1^2-m_2^2}{\omega^2-Q^2}\right)+\chi$

Table 1. Energies for $\mathcal{P}^A_z$ in each region for $m_1 < m_2$

Region	$\frac{m_1^2-m_2^2}{\omega^2-Q^2}$	$E^A_{\mathbf{p}}(m_1)$	$E^A_{\mathbf{p+q}}(m_2)$
1	$1 > ... > 0$	$\frac{1}{2}\omega\left(1+\frac{m_1^2-m_2^2}{\omega^2-Q^2}\right)-\chi$	$\frac{1}{2}\omega\left(1-\frac{m_1^2-m_2^2}{\omega^2-Q^2}\right)+\chi$
2	$... > +1$	$\frac{1}{2}\omega\left(1+\frac{m_1^2-m_2^2}{\omega^2-Q^2}\right)-\chi$	$-\frac{1}{2}\omega\left(1-\frac{m_1^2-m_2^2}{\omega^2-Q^2}\right)-\chi$
3	$... < 0$	$\chi-\frac{1}{2}\omega\left(1+\frac{m_1^2-m_2^2}{\omega^2-Q^2}\right)$	$\frac{1}{2}\omega\left(1-\frac{m_1^2-m_2^2}{\omega^2-Q^2}\right)+\chi$

Table 2. Energies for $\mathcal{P}^A_z$ in each region for $m_1 > m_2$

	$\mathcal{P}_z$	$E_{\mathbf{p}}(m_1)$	Reg.	Process	Eq.
A	$-\frac{1}{2}Q\left(1+\frac{m_1^2-m_2^2}{\omega^2-Q^2}\right)+\frac{\omega}{Q}\chi$	$\chi-\frac{1}{2}\omega\left(1+\frac{m_1^2-m_2^2}{\omega^2-Q^2}\right)$	2,3	Cerenkov	112
B	$-\frac{1}{2}Q\left(1+\frac{m_1^2-m_2^2}{\omega^2-Q^2}\right)-\frac{\omega}{Q}\chi$	$-\frac{1}{2}\omega\left(1+\frac{m_1^2-m_2^2}{\omega^2-Q^2}\right)-\chi$	2	Cerenkov	112
C	$+\frac{1}{2}Q\left(1+\frac{m_1^2-m_2^2}{\omega^2-Q^2}\right)+\frac{\omega}{Q}\chi$	$\frac{1}{2}\omega\left(1+\frac{m_1^2-m_2^2}{\omega^2-Q^2}\right)+\chi$	1 3	Pair Cerenkov	111 110
D	$+\frac{1}{2}Q\left(1+\frac{m_1^2-m_2^2}{\omega^2-Q^2}\right)-\frac{\omega}{Q}\chi$	$\frac{1}{2}\omega\left(1+\frac{m_1^2-m_2^2}{\omega^2-Q^2}\right)-\chi$	1	Pair	111

Table 3. Energies in each region for $m_1 < m_2$

	$\mathcal{P}_z$	$E_{\mathbf{p}}(m_1)$	Reg.	Process	Eq.
A	$-\frac{1}{2}\mathcal{Q}\left(1+\frac{m_1^2-m_2^2}{\omega^2-\mathcal{Q}^2}\right)+\frac{\omega}{\mathcal{Q}}\chi$	$\chi-\frac{1}{2}\omega\left(1+\frac{m_1^2-m_2^2}{\omega^2-\mathcal{Q}^2}\right)$	3	Cerenkov	112
B	$-\frac{1}{2}\mathcal{Q}\left(1+\frac{m_1^2-m_2^2}{\omega^2-\mathcal{Q}^2}\right)-\frac{\omega}{\mathcal{Q}}\chi$		None		
C	$+\frac{1}{2}\mathcal{Q}\left(1+\frac{m_1^2-m_2^2}{\omega^2-\mathcal{Q}^2}\right)+\frac{\omega}{\mathcal{Q}}\chi$	$\frac{1}{2}\omega\left(1+\frac{m_1^2-m_2^2}{\omega^2-\mathcal{Q}^2}\right)+\chi$	1 2,3	Pair Cerenkov	111 110
D	$+\frac{1}{2}\mathcal{Q}\left(1+\frac{m_1^2-m_2^2}{\omega^2-\mathcal{Q}^2}\right)-\frac{\omega}{\mathcal{Q}}\chi$	$\frac{1}{2}\omega\left(1+\frac{m_1^2-m_2^2}{\omega^2-\mathcal{Q}^2}\right)-\chi$	1 2	Pair Cerenkov	111 110

Table 4. Energies in each region for $m_1 > m_2$

the Cerenkov processes given by equations (112) and (110) have solutions given by $\mathcal{P}_z^A$ and $\mathcal{P}_z^C$. For ω and $\mathcal{Q}$ in Region 2 the solutions to the Cerenkov processes given by equations (112) and (110) depend on the relative magnitude of the masses.

The delta functions of energy given in equation (109) can be converted to delta functions of $\mathcal{P}_z$ using the tabulated results and

$$\delta(f(\mathcal{P}_z)) = \sum_i \left|\frac{df(\mathcal{P}_z^i)}{d\mathcal{P}_z}\right|^{-1} \delta(\mathcal{P}_z - \mathcal{P}_z^i), \tag{125}$$

where $\mathcal{P}_z^i$ are the solutions to the energy equation.

Hence, for $m_1 < m_2$, the delta functions arising from equations (112), (110) and (111) respectively are

$$\begin{aligned}
&\delta(E_{\mathbf{p}}(m_1) + \omega - E_{\mathbf{p+q}}(m_2)) \\
&\quad = \frac{1}{\mathcal{Q}\chi|1-\omega^2/\mathcal{Q}^2|} \\
&\qquad \times \Bigg\{ E^A_{\mathbf{p}}(m_1) E^A_{\mathbf{p+q}}(m_2) \delta(\mathcal{P}_z - \mathcal{P}_z^A)\theta\left(\sqrt{\mathcal{Q}^2 + z_2^2} - \omega\right) \\
&\qquad + E^B_{\mathbf{p}}(m_1) E^B_{\mathbf{p+q}}(m_2) \delta(\mathcal{P}_z - \mathcal{P}_z^B) \left[\theta\left(\sqrt{\mathcal{Q}^2 + z_2^2} - \omega\right) - \theta(\mathcal{Q} - \omega)\right]\Bigg\},
\end{aligned} \tag{126}$$

$$\begin{aligned}
&\delta(E_{\mathbf{p}}(m_1) - \omega - E_{\mathbf{p-q}}(m_2)) \\
&\quad = \frac{1}{\mathcal{Q}\chi|1-\omega^2/\mathcal{Q}^2|} E^C_{\mathbf{p}}(m_1) E^C_{\mathbf{p-q}}(m_2) \delta(\mathcal{P}_z - \mathcal{P}_z^C)\theta(\mathcal{Q} - \omega),
\end{aligned} \tag{127}$$

$$\begin{aligned}
&\delta(E_{\mathbf{p}}(m_1) - \omega + E_{\mathbf{p}-\mathbf{q}}(m_2)) \\
&= \frac{1}{\mathcal{Q}\chi|1-\omega^2/\mathcal{Q}^2|}\left\{E^C_{\mathbf{p}}(m_1)E^C_{\mathbf{p}-\mathbf{q}}(m_2)\delta(\mathcal{P}_z - \mathcal{P}^C_z)\theta\left(\omega - \sqrt{\mathcal{Q}^2 + z_1^2}\right)\right. \\
&\qquad\left. + E^D_{\mathbf{p}}(m_1)E^D_{\mathbf{p}-\mathbf{q}}(m_2)\delta(\mathcal{P}_z - \mathcal{P}^D_z)\theta\left(\omega - \sqrt{\mathcal{Q}^2 + z_1^2}\right)\right\},
\end{aligned} \tag{128}$$

where step functions are used to confine the solutions to the applicable regions. The energies for each region are not shown explicitly as they will cancel out when inserted in equation (109).

For $m_1 > m_2$, the delta functions arising from equations (112), (110) and (111) respectively are

$$\begin{aligned}
&\delta(E_{\mathbf{p}}(m_1) + \omega - E_{\mathbf{p}+\mathbf{q}}(m_2)) \\
&= \frac{1}{\mathcal{Q}\chi|1-\omega^2/\mathcal{Q}^2|}E^A_{\mathbf{p}}(m_1)E^A_{\mathbf{p}+\mathbf{q}}(m_2)\delta(\mathcal{P}_z - \mathcal{P}^A_z)\theta(\mathcal{Q} - \omega),
\end{aligned} \tag{129}$$

$$\begin{aligned}
&\delta(E_{\mathbf{p}}(m_1) - \omega - E_{\mathbf{p}-\mathbf{q}}(m_2)) \\
&= \frac{1}{\mathcal{Q}\chi|1-\omega^2/\mathcal{Q}^2|} \\
&\quad\times\left\{E^C_{\mathbf{p}}(m_1)E^C_{\mathbf{p}-\mathbf{q}}(m_2)\delta(\mathcal{P}_z - \mathcal{P}^C_z)\theta\left(\sqrt{\mathcal{Q}^2 + z_2^2} - \omega\right)\right. \\
&\quad\left. + E^D_{\mathbf{p}}(m_1)E^D_{\mathbf{p}-\mathbf{q}}(m_2)\delta(\mathcal{P}_z - \mathcal{P}^D_z)\left[\theta\left(\sqrt{\mathcal{Q}^2 + z_2^2} - \omega\right) - \theta(\mathcal{Q} - \omega)\right]\right\},
\end{aligned} \tag{130}$$

$$\begin{aligned}
&\delta(E_{\mathbf{p}}(m_1) - \omega + E_{\mathbf{p}-\mathbf{q}}(m_2)) \\
&= \frac{1}{\mathcal{Q}\chi|1-\omega^2/\mathcal{Q}^2|}\left\{E^C_{\mathbf{p}}(m_1)E^C_{\mathbf{p}-\mathbf{q}}(m_2)\delta(\mathcal{P}_z - \mathcal{P}^C_z)\theta\left(\omega - \sqrt{\mathcal{Q}^2 + z_1^2}\right)\right. \\
&\qquad\left. + E^D_{\mathbf{p}}(m_1)E^D_{\mathbf{p}-\mathbf{q}}(m_2)\delta(\mathcal{P}_z - \mathcal{P}^D_z)\theta\left(\omega - \sqrt{\mathcal{Q}^2 + z_1^2}\right)\right\}.
\end{aligned} \tag{131}$$

These delta functions are inserted into the expression for the polarisation tensor to give

$$\begin{aligned}
&\mathrm{Im}\, Z^J_{pp}[m_1, m_2, \mu_1] \\
&= -\frac{1}{8q^2}\left(1 + \frac{m_1^2 - m_2^2}{\omega^2 - \mathcal{Q}^2}\right)^{-1}\frac{1}{4\pi\mathcal{Q}}\int_0^\infty \frac{\mathcal{P}_\perp d\mathcal{P}_\perp}{\chi|1-\omega^2/\mathcal{Q}^2|} \\
&\qquad\times\int_{-\infty}^{\infty} d\mathcal{P}_z F(E_{\mathbf{p}}(m_1), \mu_1) Z^J_{pp}[\mathcal{P}_z, \mathcal{P}_\perp] \\
&\quad\times\left\{-\theta\left(\omega - \sqrt{\mathcal{Q}^2 + z_1^2}\right)[\delta(\mathcal{P}_z - \mathcal{P}^C_z) + \delta(\mathcal{P}_z - \mathcal{P}^D_z)]\right.
\end{aligned}$$

$$
\begin{aligned}
&+\left[\theta\left(\sqrt{\mathcal{Q}^2+z_2^2}-\omega\right)-\theta(\mathcal{Q}-\omega)\right]\theta(m_1-m_2)\\
&\qquad\qquad\times\left[\delta(\mathcal{P}_z-\mathcal{P}_z^C)+\delta(\mathcal{P}_z-\mathcal{P}_z^D)\right]\\
&-\left[\theta\left(\sqrt{\mathcal{Q}^2+z_2^2}-\omega\right)-\theta(\mathcal{Q}-\omega)\right]\theta(m_2-m_1)\\
&\qquad\qquad\times\left[\delta(\mathcal{P}_z-\mathcal{P}_z^A)+\delta(\mathcal{P}_z-\mathcal{P}_z^B)\right]\\
&+\theta(\mathcal{Q}-\omega)\left[\delta(\mathcal{P}_z-\mathcal{P}_z^C)-\delta(\mathcal{P}_z-\mathcal{P}_z^A)\right]\Bigg\}.
\end{aligned}
\tag{132}
$$

The integrals over the delta functions is performed and the energies for each $\mathcal{P}_z^i$ expression are used. This gives

$$
\begin{aligned}
&\mathrm{Im}\ Z_{pp}^J[m_1,m_2,\mu_1]\\
&= -\frac{1}{8q^2}\left(1+\frac{m_1^2-m_2^2}{\omega^2-\mathcal{Q}^2}\right)^{-1}\frac{1}{4\pi\mathcal{Q}}\int_0^\infty\frac{\mathcal{P}_\perp d\mathcal{P}_\perp}{\chi|1-\omega^2/\mathcal{Q}^2|}\\
&\quad\times\Bigg\{-\theta\left(\omega-\sqrt{\mathcal{Q}^2+z_1^2}\right)\\
&\qquad\qquad\times\left(Z_{pp}^J[\mathcal{P}_z^C,\mathcal{P}_\perp]F\left[\tfrac{1}{2}\omega\left(1+\tfrac{m_1^2-m_2^2}{\omega^2-\mathcal{Q}^2}\right)+\chi,\mu_1\right]\right.\\
&\qquad\qquad\quad\left.+Z_{pp}^J[\mathcal{P}_z^D,\mathcal{P}_\perp]F\left[\tfrac{1}{2}\omega\left(1+\tfrac{m_1^2-m_2^2}{\omega^2-\mathcal{Q}^2}\right)-\chi,\mu_1\right]\right)\\
&\quad+\left[\theta\left(\sqrt{\mathcal{Q}^2+z_2^2}-\omega\right)-\theta(\mathcal{Q}-\omega)\right]\theta(m_1-m_2)\\
&\qquad\qquad\times\left(Z_{pp}^J[\mathcal{P}_z^C,\mathcal{P}_\perp]F\left[\tfrac{1}{2}\omega\left(1+\tfrac{m_1^2-m_2^2}{\omega^2-\mathcal{Q}^2}\right)+\chi,\mu_1\right]\right.\\
&\qquad\qquad\quad\left.+Z_{pp}^J[\mathcal{P}_z^D,\mathcal{P}_\perp]F\left[\tfrac{1}{2}\omega\left(1+\tfrac{m_1^2-m_2^2}{\omega^2-\mathcal{Q}^2}\right)-\chi,\mu_1\right]\right)\\
&\quad-\left[\theta\left(\sqrt{\mathcal{Q}^2+z_2^2}-\omega\right)-\theta(\mathcal{Q}-\omega)\right]\theta(m_2-m_1)\\
&\qquad\qquad\times\left(Z_{pp}^J[\mathcal{P}_z^A,\mathcal{P}_\perp]F\left[-\tfrac{1}{2}\omega\left(1+\tfrac{m_1^2-m_2^2}{\omega^2-\mathcal{Q}^2}\right)+\chi,\mu_1\right]\right.\\
&\qquad\qquad\quad\left.+Z_{pp}^J[\mathcal{P}_z^B,\mathcal{P}_\perp]F\left[-\tfrac{1}{2}\omega\left(1+\tfrac{m_1^2-m_2^2}{\omega^2-\mathcal{Q}^2}\right)-\chi,\mu_1\right]\right)\\
&\quad+\theta(\mathcal{Q}-\omega)\times\left(Z_{pp}^J[\mathcal{P}_z^C,\mathcal{P}_\perp]F\left[\chi+\tfrac{1}{2}\omega\left(1+\tfrac{m_1^2-m_2^2}{\omega^2-\mathcal{Q}^2}\right),\mu_1\right]\right.\\
&\qquad\qquad\quad\left.-Z_{pp}^J[\mathcal{P}_z^A,\mathcal{P}_\perp]F\left[\chi-\tfrac{1}{2}\omega\left(1+\tfrac{m_1^2-m_2^2}{\omega^2-\mathcal{Q}^2}\right),\mu_1\right]\right)\Bigg\}.
\end{aligned}
\tag{133}
$$

The integration variable is changed to χ using

$$
\frac{d\chi}{d\mathcal{P}_\perp}=\frac{\mathcal{P}_\perp}{\chi(1-\omega^2/\mathcal{Q}^2)}.
\tag{134}
$$

In region 1, defined by $\theta\left(\omega-\sqrt{Q^2+z_1}\right)$, χ is a decreasing function of $\mathcal{P}_\perp$. Hence χ ranges from χ_0 at $\mathcal{P}_\perp=0$ to 0 at an upper limit of $\mathcal{P}_\perp$. That is, the restriction of $\omega>\sqrt{Q^2+z_1}$ places an upper limit on $\mathcal{P}_\perp$, as z_1 is an increasing function of $\mathcal{P}_\perp$. While $\omega>\sqrt{Q^2+z_1|_{\mathcal{P}_\perp=0}}$ then there will be some range of $\mathcal{P}_\perp$ in which the delta function is non-zero.

In region 2, χ is still a decreasing function of $\mathcal{P}_\perp$, hence the limits on χ will be the same. The restriction $\omega<\sqrt{Q^2+z_2}$ places an upper limit on $\mathcal{P}_\perp$,as z_2 is a decreasing function of $\mathcal{P}_\perp$. While $\omega<\sqrt{Q^2+z_2|_{\mathcal{P}_\perp=0}}$ then there will be some range of $\mathcal{P}_\perp$ in which the delta function is non-zero.

In region 3, χ is an increasing function of $\mathcal{P}_\perp$, hence as $\mathcal{P}_\perp$ ranges from 0 to ∞, χ ranges from χ_0 to ∞.

Taking account of the modulus sign and rearranging the integration limits gives

$$
\begin{aligned}
&\operatorname{Im} Z^J_{pp}[m_1,m_2,\mu_1]\\
&\quad= -\frac{1}{8q^2}\left(1+\frac{m_1^2-m_2^2}{\omega^2-Q^2}\right)^{-1}\frac{1}{4\pi Q}\\
&\qquad\times\Bigg\{\theta\left(\omega-\sqrt{Q^2+(m_1+m_2)^2}\right)\\
&\qquad\qquad\times\int_0^{\chi_0}d\chi\Bigg(Z^J_{pp}[\mathcal{P}_z^C(\chi),\chi]F\left[\tfrac{1}{2}\omega\left(1+\tfrac{m_1^2-m_2^2}{\omega^2-Q^2}\right)+\chi,\mu_1\right]\\
&\qquad\qquad\qquad+Z^J_{pp}[\mathcal{P}_z^D(\chi),\chi]F\left[\tfrac{1}{2}\omega\left(1+\tfrac{m_1^2-m_2^2}{\omega^2-Q^2}\right)-\chi,\mu_1\right]\Bigg)\\
&\qquad+\left[\theta\left(\sqrt{Q^2+(m_1-m_2)^2}-\omega\right)-\theta(Q-\omega)\right]\theta(m_1-m_2)\\
&\qquad\qquad\times\int_0^{\chi_0}d\chi\Bigg(Z^J_{pp}[\mathcal{P}_z^C(\chi),\chi]F\left[\tfrac{1}{2}\omega\left(1+\tfrac{m_1^2-m_2^2}{\omega^2-Q^2}\right)+\chi,\mu_1\right]\\
&\qquad\qquad\qquad+Z^J_{pp}[\mathcal{P}_z^D(\chi),\chi]F\left[\tfrac{1}{2}\omega\left(1+\tfrac{m_1^2-m_2^2}{\omega^2-Q^2}\right)-\chi,\mu_1\right]\Bigg)\\
&\qquad-\left[\theta\left(\sqrt{Q^2+(m_1-m_2)^2}-\omega\right)-\theta(Q-\omega)\right]\theta(m_2-m_1)\\
&\qquad\qquad\times\int_0^{\chi_0}d\chi\Bigg(Z^J_{pp}[\mathcal{P}_z^A(\chi),\chi]F\left[-\tfrac{1}{2}\omega\left(1+\tfrac{m_1^2-m_2^2}{\omega^2-Q^2}\right)+\chi,\mu_1\right]\\
&\qquad\qquad\qquad+Z^J_{pp}[\mathcal{P}_z^B(\chi),\chi]F\left[-\tfrac{1}{2}\omega\left(1+\tfrac{m_1^2-m_2^2}{\omega^2-Q^2}\right)-\chi,\mu_1\right]\Bigg)\\
&\qquad-\theta(Q-\omega)\\
&\qquad\qquad\times\int_{\chi_0}^{\infty}d\chi\Bigg(Z^J_{pp}[\mathcal{P}_z^C(\chi),\chi]F\left[\chi+\tfrac{1}{2}\omega\left(1+\tfrac{m_1^2-m_2^2}{\omega^2-Q^2}\right),\mu_1\right]\\
&\qquad\qquad\qquad-Z^J_{pp}[\mathcal{P}_z^A(\chi),\chi]F\left[\chi-\tfrac{1}{2}\omega\left(1+\tfrac{m_1^2-m_2^2}{\omega^2-Q^2}\right),\mu_1\right]\Bigg)\Bigg\}.
\end{aligned}
\tag{135}
$$

4.4 Polarisation Response Functions

The result given in equation (135) can be generalised to give an expression for the imaginary part of each of the Z functions using the contractions defined in equations (58) to (75). Under each of the delta functions

$$E_{\mathbf{p}}(m_1)\mathcal{Q} - \omega\mathcal{P}_z = \begin{cases} +\mathcal{Q}\chi\left(1-\omega^2/\mathcal{Q}^2\right) & \text{for } \mathcal{P}_z^A, \mathcal{P}_z^C, \\ -\mathcal{Q}\chi\left(1-\omega^2/\mathcal{Q}^2\right) & \text{for } \mathcal{P}_z^B, \mathcal{P}_z^D, \end{cases} \tag{136}$$

$$p\cdot q = \begin{cases} -\frac{1}{2}q^2\left[1+\frac{m_1^2-m_2^2}{\omega^2-\mathcal{Q}^2}\right] & \text{for } \mathcal{P}_z^A, \mathcal{P}_z^B, \\ +\frac{1}{2}q^2\left[1+\frac{m_1^2-m_2^2}{\omega^2-\mathcal{Q}^2}\right] & \text{for } \mathcal{P}_z^C, \mathcal{P}_z^D, \end{cases} \tag{137}$$

$$\mathcal{P}_\perp^2 = \left(1-\omega^2/\mathcal{Q}^2\right)\left(\chi^2-\chi_0^2\right), \tag{138}$$

where

$$\chi_0 \equiv \chi\Big|_{\mathcal{P}_\perp=0} = \sqrt{\tfrac{1}{4}\mathcal{Q}^2\left[1+\frac{m_1^2-m_2^2}{\omega^2-\mathcal{Q}^2}\right]^2+\frac{m_1^2}{1-\omega^2/\mathcal{Q}^2}}. \tag{139}$$

Hence we have

$$Z_g^T(\mathcal{P}_z^i(\chi),\chi) = 1, \tag{140}$$

$$Z_{pp}^T(\mathcal{P}_z^i(\chi),\chi) = -\tfrac{1}{2}\left(1-\omega^2/\mathcal{Q}^2\right)\left(\chi^2-\chi_0^2\right), \tag{141}$$

$$Z_g^L(\mathcal{P}_z^i(\chi),\chi) = 1, \tag{142}$$

$$Z_{pp}^L(\mathcal{P}_z^i(\chi),\chi) = -\frac{q^2}{\mathcal{Q}^2}\chi^2, \tag{143}$$

$$Z_g^Q(\mathcal{P}_z^i(\chi),\chi) = 1, \tag{144}$$

$$Z_{pp}^Q(\mathcal{P}_z^i(\chi),\chi) = \tfrac{1}{4}q^2\left[1+\frac{m_1^2-m_2^2}{\omega^2-\mathcal{Q}^2}\right]^2, \tag{145}$$

$$Z_{pq}^Q(\mathcal{P}_z^i(\chi),\chi) = \tfrac{1}{2}q^4\left[1+\frac{m_1^2-m_2^2}{\omega^2-\mathcal{Q}^2}\right]^2, \tag{146}$$

$$Z_{qq}^Q(\mathcal{P}_z^i(\chi),\chi) = q^2, \tag{147}$$

$$Z_{pp}^C(\mathcal{P}_z^i(\chi),\chi) = \begin{cases} -\omega\chi\left(1-\omega^2/\mathcal{Q}^2\right)\left[1+\frac{m_1^2-m_2^2}{\omega^2-\mathcal{Q}^2}\right] & \text{for } \mathcal{P}_z^A, \mathcal{P}_z^D, \\ +\omega\chi\left(1-\omega^2/\mathcal{Q}^2\right)\left[1+\frac{m_1^2-m_2^2}{\omega^2-\mathcal{Q}^2}\right] & \text{for } \mathcal{P}_z^B, \mathcal{P}_z^C, \end{cases} \tag{148}$$

$$Z_{pq}^C(\mathcal{P}_z^i(\chi),\chi) = q^2 Z_{pp}^C(\mathcal{P}_z^i(\chi),\chi), \tag{149}$$

and the imaginary part of a particular Z function is obtained by substituting the expression for $Z(\mathcal{P}_z^i(\chi),\chi)$ in equation (135). The $Z(\mathcal{P}_z^i(\chi),\chi)$ functions not explicitly shown here are identically zero.

5 Grand Table of Results

The aim of the two papers in this series is to calculate the finite temperature self-energy polarisation tensor for the electroweak model in the R_ξ gauge. The polarisation tensor is expressed in terms of the basis tensors and the polarisation response functions. The diagrammatic expansion has been used and the diagrams needed for the calculation of the photon polarisation tensor to e^2 order are

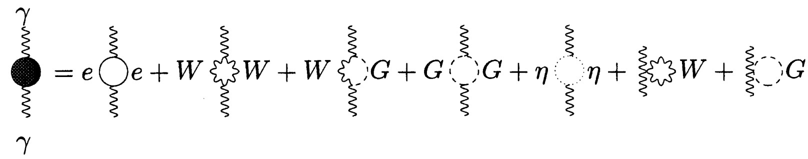

The diagrams needed for the calculation of the Z boson polarisation tensor to g^2 order are

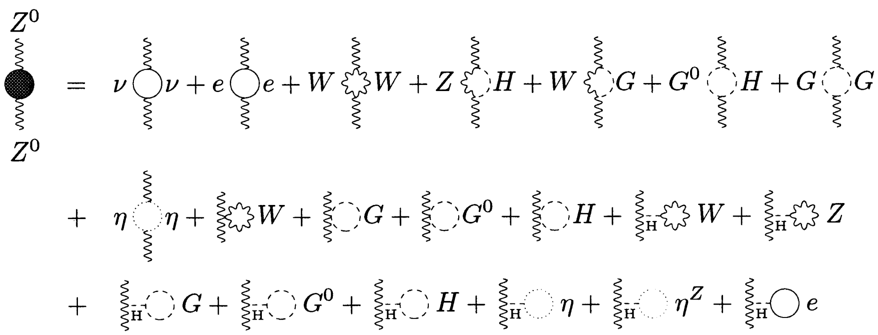

The diagrams needed for the calculation of the W boson polarisation tensor to g^2 order are

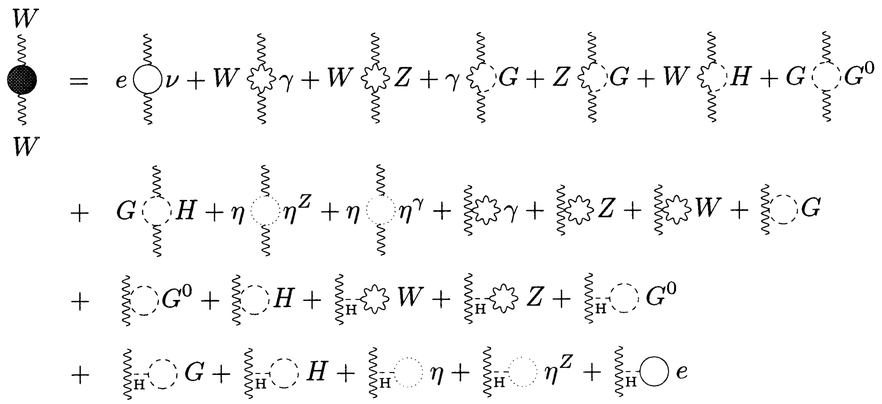

In view of the great number of Feynman diagrams that are taken into account, the calculations have been arranged systematically and this is shown in Table 5. In this table each generic type of diagram is shown along with the equation number for the polarisation response functions, the table in Paper I which tabulates the vertex factors relevant to this diagram and the list of Y and Z functions used to describe the polarisation response functions where J is one of $\{T, L, Q, C\}$.

In Table 6, the equation number for the real and imaginary parts for each Y and Z function is given. The Y functions all have an imaginary part that is identically zero. Some Y and Z functions are identically zero due to orthogonality between tensors.

Diagram	Equation for polarisation response functions	Vertex factor from Paper I	Y and Z functions
	(B4)	Table A1	$Y_g^J, Z_g^J, Z_{pp}^J, Z_{pq}^J$
	(B9), (B10) (B11), (B12)	Table A2	$Y_g^J, Y_{pp}^J, Y_{qq}^J$ $Z_g^J, Z_{pp}^J, Z_{pq}^J, Z_{qq}^J$
	(B5)	Table A3	Z_{pp}^J, Z_{pq}^J
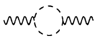	(B6)	Table A4	$Z_{pp}^J, Z_{pq}^J, Z_{qq}^J$
	(B7), (B8)	Table A5	$Z_g^J, Z_{pp}^J, Z_{pq}^J, Z_{qq}^J$
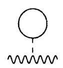	(B14)	Table A5, B1	Y_g^J
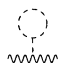	(B13)	Table A5, B2	Y_g^J
	(B15)	Table A5, B3	Y_g^J
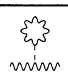	(B16)	Table A5	Y_g^J
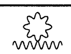	(B2), (B3)	Table C0	Y_g^J, Y_{pp}^J
	(B1)	Table C1	Y_g^J

Table 5. Grand table of diagrams

Function	T		L		Q		C	
	Im	Re	Im	Re	Im	Re	Im	Re
Y_g	zero	(77)	zero	(89)	zero	(93)	zero	zero
Y_{pp}	zero	(78)	zero	(90)	zero	(94)	zero	(100)
Y_{qq}	zero	zero	zero	zero	zero	(95)	zero	zero
Z_g	(140)	(85)	(142)	(91)	(144)	(96)	zero	zero
Z_{pp}	(141)	(86)	(143)	(92)	(145)	(97)	(148)	(101)
Z_{pq}	zero	zero	zero	zero	(146)	(98)	(149)	(102)
Z_{qq}	zero	zero	zero	zero	(147)	(99)	zero	zero

Table 6. Grand table of Y and Z functions

6 Summary and Discussion

For the standard electroweak theory of (Glashow 1961; Salam 1968; Weinberg 1967) the finite temperature part of the polarisation tensor for the $W^{\pm}$, Z^0 and γ gauge bosons has been calculated in a systematic manner using gauge field theory and the R_ξ gauge. The polarisation tensor gives the shift in the propagator of the gauge bosons due to interactions and is expressed in terms of the polarisation response functions which are given by π^T, π^L, π^Q and π^C.

Finite temperature field theory is used in the imaginary-time formalism which means that the perturbation expansion used for the zero temperature theory can be carried over to the finite temperature calculations under the application of the finite temperature Feynman rules. These rules prescribe a Matsubara summation due to the periodic boundary conditions.

The contributions to the polarisation tensor due to the interactions described by the electroweak model are expressed in terms of Feynman diagrams. Each Feynman diagram is one of three distinct types—loop, tadpole or balloon—and for each of these types, a procedure is given to calculate the contribution of the general diagram. This procedure is followed for the combinations of particles possible for each diagram and the results for the general case are given in the Appendices. By calculating the Feynman diagrams in this systematic manner the symmetries of the system are exploited and the results for each diagram can be constructed from a particular set of functions, which can then be cross referenced.

The full set of tensors used to describe the polarisation tensor have been examined and the propagator for the gauge bosons in the presence of interactions has been obtained. Ward's identity has been applied and this yields a relationship between the polarisation response functions which are given by π^T, π^L, π^Q and π^C.

The leading characteristics of the electroweak plasma, in particular the mode structure, can in principle be developed from a knowledge of the real part of the polarisation tensor. In Section 3 the real part of the Y and Z functions has been expressed in terms of the Y and Z functions.

The calculation of the imaginary part of the polarisation tensor gives the dissipative processes occurring in the plasma and these processes are defined by the equations of energy and momentum conservation. For the electroweak theory the particles propagating in the loop diagram may be different and the solution procedure used for the equations of energy and momentum conservation has to be extended from the results of the QED case given by Tsytovich (1961). This leads to damping regions dependent on the masses of the particles propagating in the diagram.

The correspondence between each diagram and the equations and functions used to describe it is given in Table 5 of the present paper.

7 Further Work

With the techniques available as detailed in previous sections the way is now open for the future study of the physical properties of the electroweak system. The polarisation tensor corresponding to the propagation of a particular gauge boson has been obtained by adding together the contributions from the appropriate Feynman diagrams. This has been done in the high temperature limit by considering the high temperature expansions of the Y and Z functions and will appear in a subsequent paper. This will show the ξ independence of the polarisation tensor in the high temperature limit for the electroweak system.

The most immediate use of this work would be the calculation of dispersion relations which would provide information about the modes and damping for the propagation of particles through the system. Physical properties such as the modes of propagation, damping, excitations and screening length in the plasma could all be considered. The classical field equations could be calculated from the electroweak Lagrangian by the Euler–Lagrange equations for each field and then linearised, where each field would be expanded as a classical part and a fluctuation part and only first order terms in the fluctuations would be kept. The one-loop contributions would be used for the fluctuations and the classical field equations solved. The solutions to the classical field equations give the equilibrium state of the plasma about which the fluctuations yield the modes, excitations and quasi-particles. Comparison of these properties with those expected from the QED case would be of great interest.

8 Acknowledgments

One of us (BJKS) would like to acknowledge the support of an Australian Post-Graduate Research Award. This work was completed with the assistance of an Australian Research Council award.

References

Bailin, D., and Love, A. (1986). 'Introduction to Gauge Field Theory' (Adam Hilger: Bristol).

Carrington, M. E. (1992). *Phys. Rev.* D **45**, 2933.

Glashow, S. L. (1961). *Nucl. Phys.* **22**, 579.

Gross, D. J., Pisarski, R. D., and Yaffe, L. G. (1981). *Rev. Mod. Phys.* **53**, 43.

Haber, H. E., and Weldon, H. A. (1982*a*). *Phys. Rev.* D **25**, 502.

Haber, H. E., and Weldon, H. A. (1982*b*). *J. Math. Phys.* **23**, 1852.

Hsieh, A., and Yehudai, E. (1992). *Comput. Phys.* **6**, 253.

Itzykson, C., and Zuber, J. B. (1980). 'Quantum Field Theory' (McGraw–Hill: New York).

Kapusta, J. I. (1989). 'Finite Temperature Field Theory' (Cambridge University Press: New York).

Melrose, D. B. (1982). *Aust. J. Phys.* **35**, 41.

Melrose, D. B., and McPhedran, R. C. (1993). 'Electromagnetic Processes in Dispersive Media' (Cambridge University Press: New York).

Salam, A. (1968). *In* 'Elementary Particle Physics (Nobel Symp. No. 8)' (Ed. N. Svartholm) (Almqvist and Wilsell).

Smith, B. J. K., Witte, N. S., and Hines, K. C. (1995). *Aust. J. Phys.* **48**, 739.

Tsytovich, V. N. (1961). *Sov. Phys. JETP* **13**, 1249.

Weinberg, S. (1967). *Phys. Rev. Lett.* **19**, 1264.

Wolfram, S. (1991). 'Mathematica—A System for Doing Mathematics by Computer', 2nd ed. (Addison–Wesley: Redwood City, California).

A Notation

The notation used in this work is standard (except for the labelling used for the vertices) and is given in Paper I.

A.1 Photon Mass

The finite temperature photon propagator is

$$\frac{1}{p^2}\left[g_{\alpha\beta}-(1-\xi)\frac{p_\alpha p_\beta}{p^2}\right], \tag{A1}$$

while the finite temperature propagator for a general gauge boson is

$$\left(g_{\alpha\beta}-\frac{p_\alpha p_\beta}{m^2}\right)\left[p^{o2}-E^2_{\mathbf{p}}(m)\right]^{-1}+\frac{p_\alpha p_\beta}{m^2}\left[p^{o2}-E^2_{\mathbf{p}}(\xi^{\frac{1}{2}}m)\right]^{-1}. \tag{A2}$$

For a photon propagating in the loop of a diagram the result for that general diagram is used with the transformation $\xi^{\frac{1}{2}}m_\gamma \to m_\gamma$ made only in the Y and Z functions and then the high temperature expansion is performed. This reproduces the form expected. The same transformation in the whole expression totally removes the ξ dependence from the result.

B Polarisation Response Functions

The procedure given in this paper and Paper I has been used to calculate the $\mathcal{K}_i$ and $\mathcal{M}_i$ constants and equations (56), (55) and (57) have been recast using these constants to give the polarisation response functions for the tadpole, loop and balloon diagrams respectively. The $\mathcal{K}_i$ and $\mathcal{M}_i$ constants are not given explicitly. The generic superscript J is used where J is one of $\{T, L, Q, C\}$.

B.1 Tadpole: Higgs

Diagram: 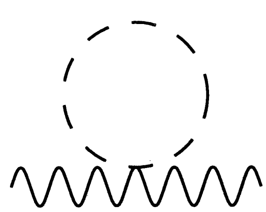

Vertex: $\mathcal{C}_1 g_{\mu\nu}$

Propagator: $-\left[p^{o2}-E^2_{\mathbf{p}}(m_1)\right]^{-1}.$

The polarisation response functions are given by

$$\pi^J = \mathcal{C}_1 Y^J_g[m_1, \mu_1]. \tag{B1}$$

B.2 Tadpole: Gauge

Diagram: 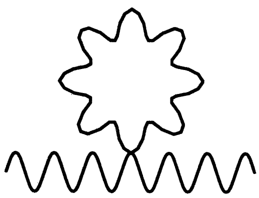

Vertex: $\mathcal{C}_0\left[2g_{\mu\nu}g_{\alpha\beta} - g_{\mu\alpha}g_{\nu\beta} - g_{\mu\beta}g_{\nu\alpha}\right]$

The polarisation response functions for this diagram consists of 2 parts, corresponding to the 2 parts of the gauge boson propagator. The first part of the gauge boson propagator is

$$\text{Propagator:} \qquad \left(g_{\alpha\beta} - \frac{p_\alpha p_\beta}{m_1^2}\right)\left[p^{\text{o}2} - E^2_{\mathbf{p}}(m_1)\right]^{-1}.$$

The polarisation response functions for this part are

$$\pi_1^J = -2\mathcal{C}_0\left\{2Y_g^J[m_1,\mu_1] + \frac{1}{m_1^2}Y_{pp}^J[m_1,\mu_1]\right\}. \tag{B2}$$

The second part of the gauge boson propagator is

$$\text{Propagator:} \qquad \frac{p_\alpha p_\beta}{m_1^2}\left[p^{\text{o}2} - E^2_{\mathbf{p}}(\xi^{\frac{1}{2}}m_1)\right]^{-1}.$$

The polarisation response functions for this part are

$$\pi_2^J = 2\mathcal{C}_0\left\{-\xi Y_g^J[\xi^{\frac{1}{2}}m_1,\mu_1] + \frac{1}{m_1^2}Y_{pp}^J[\xi^{\frac{1}{2}}m_1,\mu_1]\right\}. \tag{B3}$$

The total expression for π^J is the sum of the two parts.

For the $W^\pm$ tadpole contribution to the $W^\pm$ polarisation tensor, some care will be required in selecting the correct legs of the vertex to contract together. This effectively will multiply the expression by $-\frac{1}{2}$.

B.3 Loop: Fermion–Fermion

Diagram: 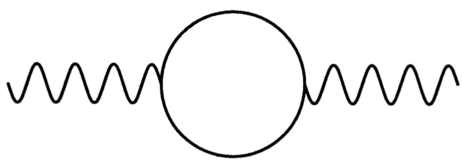

Vertex1: $\gamma_\mu(\mathcal{A}_0\mathbf{I} + \mathcal{A}_1\gamma_5)$

$$
\begin{aligned}
\text{Propagator1:} \quad & -\left(\not{p}+m_1\right)\left[p^{o2}-E^2_{\mathbf{p}}(m_1)\right]^{-1}\\
\text{Propagator2:} \quad & -\left(\not{p}'+m_2\right)\left[p^{o'^2}-E^2_{\mathbf{p}'}(m_2)\right]^{-1}\\
\text{Vertex2:} \quad & \gamma_\nu(\mathcal{A}_0'\mathbf{I}+\mathcal{A}_1'\gamma_5).
\end{aligned}
$$

When the expression for this diagram is calculated a trace over the gamma matrices is performed. The anti-symmetry of the γ matrices is the reason that the expression for π^J is not proportional to the $\mathcal{A}_0\mathcal{A}_0'+\mathcal{A}_1\mathcal{A}_1'$ combination. The polarisation response functions are

$$
\begin{aligned}
\pi^J \;=\; & Y^J_g[m_1,\mu_1]2(\mathcal{A}_0\mathcal{A}_0'+\mathcal{A}_1\mathcal{A}_1')\\
+\; & Z^J_g[m_1,m_2,\mu_1]2(q^2+m_1^2-m_2^2)\\
& \times\left(\mathcal{A}_0\mathcal{A}_0'\left[q^2-(m_1-m_2)^2\right]+\mathcal{A}_1\mathcal{A}_1'\left[q^2-(m_1+m_2)^2\right]\right)\\
+\; & Z^J_{pp}[m_1,m_2,\mu_1]8(q^2+m_1^2-m_2^2)(\mathcal{A}_0\mathcal{A}_0'+\mathcal{A}_1\mathcal{A}_1')\\
-\; & Z^J_{pq}[m_1,m_2,\mu_1]8(\mathcal{A}_0\mathcal{A}_0'+\mathcal{A}_1\mathcal{A}_1')\\
+\; & m_1\leftrightarrow m_2,\mu_1\leftrightarrow\mu_2.
\end{aligned}
\tag{B4}
$$

B.4 Loop: Ghost–Ghost

Diagram: 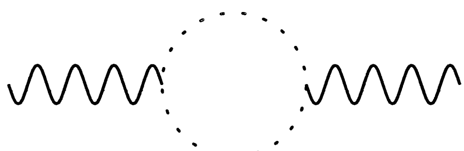

$$
\begin{aligned}
\text{Vertex1:} \quad & \mathcal{A}_3 p_\mu\\
\text{Propagator1:} \quad & -\left[p^{o2}-E^2_{\mathbf{p}}(m_1)\right]^{-1}\\
\text{Propagator2:} \quad & -\left[p^{o'^2}-E^2_{\mathbf{p}'}(m_2)\right]^{-1}\\
\text{Vertex2:} \quad & \mathcal{A}_3' p_\nu'.
\end{aligned}
$$

The polarisation response functions are given by

$$
\begin{aligned}
\pi^J \;=\; \mathcal{A}_3\mathcal{A}_3'\Big\{ & -Z^J_{pp}[m_1,m_2,\mu_1](q^2+m_1^2-m_2^2)\\
& -Z^J_{pp}[m_2,m_1,\mu_1](q^2+m_2^2-m_1^2)\\
& +2Z^J_{pq}[m_1,m_2,\mu_1]\Big\}.
\end{aligned}
\tag{B5}
$$

B.5 Loop: Higgs–Higgs

Diagram: 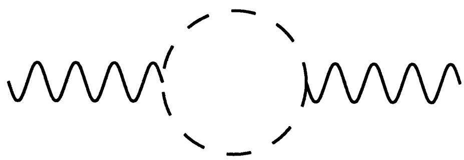

$$\begin{aligned}
\text{Vertex1:} \quad & \mathcal{A}_4(p+p')_\mu \\
\text{Propagator1:} \quad & -\left[p^{o2} - E^2_{\mathbf{p}}(m_1)\right]^{-1} \\
\text{Propagator2:} \quad & -\left[p^{o'2} - E^2_{\mathbf{p}'}(m_2)\right]^{-1} \\
\text{Vertex2:} \quad & \mathcal{A}'_4(p'+p)_\nu .
\end{aligned}$$

The polarisation response functions are given by

$$\begin{aligned}
\pi^J \quad = \quad & \mathcal{A}_4\mathcal{A}'_4\Big\{4Z^J_{pp}[m_1, m_2, \mu_1](q^2+m_1^2-m_2^2) \\
& -4Z^J_{pq}[m_1, m_2, \mu_1] \\
& +Z^J_{qq}[m_1, m_2, \mu_1](q^2+m_1^2-m_2^2)\Big\} \\
+ \quad & m_1 \leftrightarrow m_2, \mu_1 \leftrightarrow \mu_2 .
\end{aligned} \tag{B6}$$

B.6 Loop: Gauge–Higgs

Diagram: 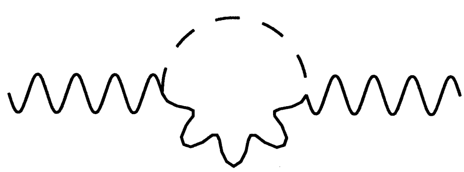

$$\begin{aligned}
\text{Vertex1:} \quad & \mathcal{A}_5 g_{\mu\rho} \\
\text{Vertex2:} \quad & \mathcal{A}'_5 g_{\nu\lambda} .
\end{aligned}$$

The polarisation response function for this diagram consists of 2 parts, corresponding to the possible combinations of the gauge boson propagator and Higgs sector propagator. The first combination of propagators is

$$\begin{aligned}
\text{Propagator1:} \quad & \left(g_{\lambda\rho} - \frac{p_\lambda p_\rho}{m_1^2}\right)\left[p^{o2} - E^2_{\mathbf{p}}(m_1)\right]^{-1} \\
\text{Propagator2:} \quad & -\left[p^{o'2} - E^2_{\mathbf{p}'}(m_2)\right]^{-1} .
\end{aligned}$$

The polarisation response functions for this part are

$$\begin{aligned}\pi_1^J = \frac{\mathcal{A}_5\mathcal{A}_5'}{m_1^2}\Big\{ & -Z_g^J[m_1,m_2,\mu_1]m_1^2(q^2+m_1^2-m_2^2)\\ & +Z_{pp}^J[m_1,m_2,\mu_1](q^2+m_1^2-m_2^2)\\ & -Z_g^J[m_2,m_1,\mu_2]m_1^2(q^2+m_2^2-m_1^2)\\ & +Z_{pp}^J[m_2,m_1,\mu_2](q^2+m_2^2-m_1^2)\\ & -Z_{pq}^J[m_2,m_1,\mu_2]2\\ & +Z_{qq}^J[m_2,m_1,\mu_2](q^2+m_2^2-m_1^2)\Big\}. \end{aligned} \tag{B7}$$

The second combination of propagators is

$$\begin{aligned}&\text{Propagator1:} && \frac{p_\lambda p_\rho}{m_1^2}\left[p^{o2}-E_{\mathbf{p}}^2(\xi^{\frac{1}{2}}m_1)\right]^{-1}\\ &\text{Propagator2:} && -\left[{p^{o'}}^2-E_{\mathbf{p}'}^2(m_2)\right]^{-1}.\end{aligned}$$

The polarisation response functions for this part are

$$\begin{aligned}\pi_2^J = -\frac{\mathcal{A}_5\mathcal{A}_5'}{m_1^2}\Big\{ & Z_{pp}^J[\xi^{\frac{1}{2}}m_1,m_2,\mu_1](q^2+\xi m_1^2-m_2^2)\\ & +Z_{pp}^J[m_2,\xi^{\frac{1}{2}}m_1,\mu_2](q^2+m_2^2-\xi m_1^2)\\ & -Z_{pq}^J[m_2,\xi^{\frac{1}{2}}m_1,\mu_2]\\ & +Z_{qq}^J[m_2,\xi^{\frac{1}{2}}m_1,\mu_2](q^2+m_2^2-\xi m_1^2)\Big\}. \end{aligned} \tag{B8}$$

The total expression for π^J is the sum of the two parts.

B.7 Loop: Gauge–Gauge

Diagram: 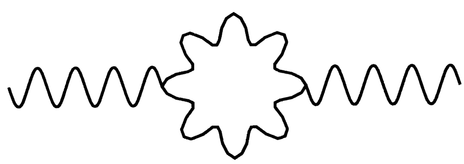

$$\begin{aligned}&\text{Vertex1:} && \mathcal{A}_2\left[(-p'-p)_\mu g_{\lambda\alpha}+(p-q')_\alpha g_{\mu\lambda}+(q'+p')_\lambda g_{\alpha\mu}\right]\\ &\text{Vertex2:} && \mathcal{A}_2'\left[(p'+q)_\rho g_{\nu\beta}+(p-q)_\beta g_{\rho\nu}+(-p'-p)_\nu g_{\beta\rho}\right].\end{aligned}$$

The polarisation response function for this diagram consists of 4 parts, corresponding to the possible combinations of the gauge boson propagators. The first combination of propagators is

$$\text{Propagator1:} \quad \left(g_{\lambda\rho}-\frac{p_\lambda p_\rho}{m_1^2}\right)\left[p^{o2}-E_{\mathbf{p}}^2(m_1)\right]^{-1}$$

$$\text{Propagator2:} \qquad \left(g_{\alpha\beta} - \frac{p'_\alpha p'_\beta}{m_2^2}\right) \left[p^{0'2} - E^2_{\mathbf{p}'}(m_2)\right]^{-1}.$$

The polarisation response functions for this part are

$$\begin{aligned}
\pi_1^J \;=\; & \frac{\mathcal{A}_2\mathcal{A}'_2}{m_1^2 m_2^2}\Big\{ Y_g^J[m_1,\mu_1](m_2^2-q^2)m_2^2 \\
& -Z_g^J[m_1,m_2,\mu_1](m_1^2+m_2^2)(q^2+m_1^2-m_2^2) \\
& \qquad \times\left[q^2-(m_1+m_2)^2\right]\left[q^2-(m_1-m_2)^2\right] \\
& -Y_{pp}^J[m_1,\mu_1]m_2^2 \\
& +Z_{pp}^J[m_1,m_2,\mu_1](q^2+m_1^2-m_2^2) \\
& \qquad \times\left[m_1^4+10m_1^2m_2^2+m_2^4-2m_1^2q^2-2m_2^2q^2+q^4\right] \\
& +Z_{pq}^J[m_1,m_2,\mu_1]\left[m_1^4-10m_1^2m_2^2-3m_2^4+4m_2^2q^2-q^4\right] \\
& +Y_{qq}^J[m_1,\mu_1]\tfrac{1}{4}(q^2+m_1^2-m_2^2) \\
& +Z_{qq}^J[m_1,m_2,\mu_1](q^2+m_1^2-m_2^2) \\
& \qquad \times\left[q^4-7m_1^4+6m_1^2q^2+m_2^2(m_2^2-14m_1^2-2q^2)\right]\Big\} \\
+ \;\; & m_1 \leftrightarrow m_2, \mu_1 \leftrightarrow \mu_2.
\end{aligned} \tag{B9}$$

The second combination of propagators is

$$\begin{aligned}
&\text{Propagator1:} && \left(g_{\lambda\rho} - \frac{p_\lambda p_\rho}{m_1^2}\right)\left[p^{02} - E^2_{\mathbf{p}}(m_1)\right]^{-1} \\
&\text{Propagator2:} && \frac{p'_\alpha p'_\beta}{m_2^2}\left[p^{0'2} - E^2_{\mathbf{p}'}(\xi^{\frac12} m_2)\right]^{-1}.
\end{aligned}$$

The polarisation response functions for this part are

$$\begin{aligned}
\pi_2^J \;=\; & \frac{\mathcal{A}_2\mathcal{A}'_2}{m_1^2 m_2^2}\Big\{ Z_g^J[m_1,\xi^{\frac12}m_2,\mu_1](q^2-m_1^2)^2 m_1^2(q^2+m_1^2-\xi m_2^2) \\
& -Z_{pp}^J[m_1,\xi^{\frac12}m_2,\mu_1](q^2-m_1^2)^2(q^2+m_1^2-\xi m_2^2) \\
& +Z_{pq}^J[m_1,\xi^{\frac12}m_2,\mu_1](q^2-m_1^2)(q^2+m_1^2-\xi m_2^2) \\
& -Y_{qq}^J[m_1,\mu_1]\tfrac14(q^2+m_1^2-\xi m_2^2) \\
& -Z_{qq}^J[m_1,\xi^{\frac12}m_2,\mu_1]\tfrac14(q^2+m_1^2-\xi m_2^2) \\
& \qquad \times\left[q^4-7m_1^4+6m_1^2q^2+\xi m_2^2(\xi m_2^2-2m_1^2-2q^2)\right] \\
& +Y_g^J[\xi^{\frac12}m_2,\mu_2](q^2-\xi m_2^2-m_1^2)m_1^2 \\
& +Z_g^J[\xi^{\frac12}m_2,m_1,\mu_2](q^2-m_1^2)^2 m_1^2(q^2+\xi m_2^2-m_1^2) \\
& +Y_{pp}^J[\xi^{\frac12}m_2,\mu_2]m_1^2
\end{aligned}$$

$$
\begin{aligned}
&-Z^J_{pp}[\xi^{\frac{1}{2}}m_2, m_1, \mu_2](q^2 - m_1^2)^2(q^2 + \xi m_2^2 - m_1^2) \\
&+Z^J_{pq}[\xi^{\frac{1}{2}}m_2, m_1, \mu_2](q^2 - m_1^2)(q^2 + \xi m_2^2 - 3m_1^2) \\
&-Y^J_{qq}[\xi^{\frac{1}{2}}m_2, \mu_2]\tfrac{1}{4}(q^2 + \xi m_2^2 - m_1^2) \\
&-Z^J_{qq}[\xi^{\frac{1}{2}}m_2, m_1, \mu_2]\tfrac{1}{4}(q^2 + \xi m_2^2 - m_1^2) \\
&\qquad\times\left[q^4 + m_1^4 - 2m_1^2q^2 + \xi m_2^2(\xi m_2^2 - 6m_1^2 + 2q^2)\right]\Bigg\}.
\end{aligned}
\tag{B10}
$$

The third combination of propagators is

$$
\begin{aligned}
&\text{Propagator1:} \quad \frac{p_\lambda p_\rho}{m_1^2}\left[p^{o2} - E^2_{\mathbf{p}}(\xi^{\frac{1}{2}}m_1)\right]^{-1} \\
&\text{Propagator2:} \quad \left(g_{\alpha\beta} - \frac{p'_\alpha p'_\beta}{m_2^2}\right)\left[p^{o\prime 2} - E^2_{\mathbf{p}'}(m_2)\right]^{-1}.
\end{aligned}
$$

The polarisation response functions for this part are

$$
\begin{aligned}
\pi^J_3 = \frac{\mathcal{A}_2\mathcal{A}'_2}{m_2^2m_1^2}\Bigg\{ &Y^J_g[\xi^{\frac{1}{2}}m_1, \mu_1](q^2 - \xi m_1^2 - m_2^2)m_2^2 \\
&+Z^J_g[\xi^{\frac{1}{2}}m_1, m_2, \mu_1](q^2 - m_2^2)^2m_2^2(q^2 + \xi m_1^2 - m_2^2) \\
&+Y^J_{pp}[\xi^{\frac{1}{2}}m_1, \mu_1]m_2^2 \\
&-Z^J_{pp}[\xi^{\frac{1}{2}}m_1, m_2, \mu_1](q^2 - m_2^2)^2(q^2 + \xi m_1^2 - m_2^2) \\
&+Z^J_{pq}[\xi^{\frac{1}{2}}m_1, m_2, \mu_1](q^2 - m_2^2)(q^2 + \xi m_1^2 - 3m_2^2) \\
&-Y^J_{qq}[\xi^{\frac{1}{2}}m_1, \mu_1]\tfrac{1}{4}(q^2 + \xi m_1^2 - m_2^2) \\
&-Z^J_{qq}[\xi^{\frac{1}{2}}m_1, m_2, \mu_1]\tfrac{1}{4}(q^2 + \xi m_1^2 - m_2^2) \\
&\qquad\times\left[q^4 + m_2^4 - 2m_2^2q^2 + \xi m_1^2(\xi m_1^2 - 6m_2^2 + 2q^2)\right] \\
&+Z^J_g[m_2, \xi^{\frac{1}{2}}m_1, \mu_2](q^2 - m_2^2)^2m_2^2(q^2 + m_2^2 - \xi m_1^2) \\
&-Z^J_{pp}[m_2, \xi^{\frac{1}{2}}m_1, \mu_2](q^2 - m_2^2)^2(q^2 + m_2^2 - \xi m_1^2) \\
&+Z^J_{pq}[m_2, \xi^{\frac{1}{2}}m_1, \mu_2](q^2 - m_2^2)(q^2 + m_2^2 - \xi m_1^2) \\
&-Y^J_{qq}[m_2, \mu_2]\tfrac{1}{4}(q^2 + m_2^2 - \xi m_1^2) \\
&-Z^J_{qq}[m_2, \xi^{\frac{1}{2}}m_1, \mu_2]\tfrac{1}{4}(q^2 + m_2^2 - \xi m_1^2) \\
&\qquad\times\left[q^4 - 7m_2^4 + 6m_2^2q^2 + \xi m_1^2(\xi m_1^2 - 2m_2^2 - 2q^2)\right]\Bigg\}.
\end{aligned}
\tag{B11}
$$

The fourth combination of propagators is

$$
\text{Propagator1:} \quad \frac{p_\lambda p_\rho}{m_1^2}\left[p^{o2} - E^2_{\mathbf{p}}(\xi^{\frac{1}{2}}m_1)\right]^{-1}
$$

$$\text{Propagator2:} \qquad \frac{p'_\alpha p'_\beta}{m_2^2}\left[p^{o\prime 2} - E^2_{\mathbf{p}'}(\xi^{\frac{1}{2}} m_2)\right]^{-1}.$$

The polarisation response functions for this part are

$$\begin{aligned}
\pi_4^J \;=\; & \frac{\mathcal{A}_2\mathcal{A}'_2}{m_2^2 m_1^2}\Big\{Z^J_{pp}[\xi^{\frac{1}{2}}m_1,\xi^{\frac{1}{2}}m_2,\mu_1]q^4(q^2+\xi m_1^2-\xi m_2^2)\\
& -Z^J_{pq}[\xi^{\frac{1}{2}}m_1,\xi^{\frac{1}{2}}m_2,\mu_1]q^2(q^2+\xi m_1^2-\xi m_2^2)\\
& +Y^J_{qq}[\xi^{\frac{1}{2}}m_1,\mu_1]\tfrac{1}{4}(q^2+\xi m_1^2-\xi m_2^2)\\
& +Z^J_{qq}[\xi^{\frac{1}{2}}m_1,\xi^{\frac{1}{2}}m_2,\mu_1]\tfrac{1}{4}(q^2+\xi m_1^2-\xi m_2^2)^3\Big\}\\
+ \;\; & m_1 \leftrightarrow m_2, \mu_1 \leftrightarrow \mu_2.
\end{aligned} \tag{B12}$$

The total expression for π^J is the sum of the four parts.

B.8 Balloon: Higgs–Higgs

Diagram: 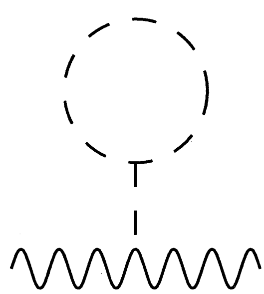

$$\begin{aligned}
\text{Propagator1:} \quad & -\left[p^{o2} - E^2_{\mathbf{p}}(m_1)\right]^{-1}\\
\text{Vertex1:}(p' \to 0) \quad & \mathcal{B}_2\\
\text{Propagator2:}(p' \to 0) \quad & 1/m_H^2\\
\text{Vertex2:}(p' \to 0) \quad & \mathcal{A}_5 g_{\mu\nu}.
\end{aligned}$$

The polarisation response functions are given by

$$\pi^J = \frac{\mathcal{B}_2\mathcal{A}_5}{m_H^2} Y^J_g[m_1,\mu_1]. \tag{B13}$$

B.9 Balloon: Higgs–Fermion

Diagram:

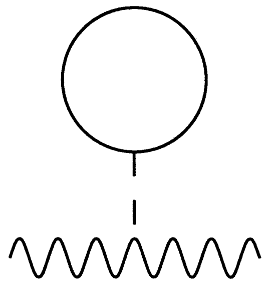

Propagator1:	$-(\not p + m_1)\left[p^{o2} - E^2_{\mathbf{p}}(m_1)\right]^{-1}$
Vertex1:$(p' \to 0)$	$\mathcal{B}_0\mathbf{I} + \mathcal{B}_1\gamma_5$
Propagator2:$(p' \to 0)$	$1/m_H^2$
Vertex2:$(p' \to 0)$	$\mathcal{A}_5 g_{\mu\nu}$.

The polarisation response functions are given by

$$\pi^J = 4\frac{\mathcal{B}_0\mathcal{A}_5}{m_H^2} m_1 Y_g^J[m_1, \mu_1]. \tag{B14}$$

B.10 Balloon: Higgs–Ghost

Diagram:

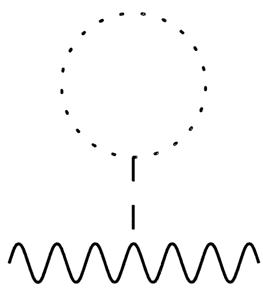

Propagator1:	$-\left[p^{o2} - E^2_{\mathbf{p}}(m_1)\right]^{-1}$
Vertex1:$(p' \to 0)$	$\mathcal{B}_3\xi$
Propagator2:$(p' \to 0)$	$1/m_H^2$
Vertex2:$(p' \to 0)$	$\mathcal{A}_5 g_{\mu\nu}$.

The polarisation response functions are given by

$$\pi^J = -\frac{\mathcal{B}_3\mathcal{A}_5}{m_H^2}\xi Y_g^J[m_1, \mu_1]. \tag{B15}$$

B.11 Balloon: Higgs–Gauge

Diagram:

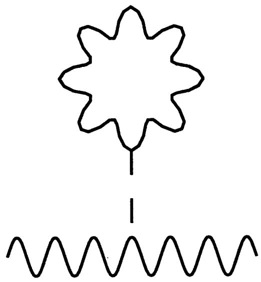

$$
\begin{array}{rl}
\text{Propagator1:} & \left(g_{\lambda\rho} - \dfrac{p_\lambda p_\rho}{m_1^2}\right)\left[p^{o2} - E^2_{\mathbf{p}}(m_1)\right]^{-1} \\
 & + \dfrac{p_\lambda p_\rho}{m_1^2}\left[p^{o2} - E^2_{\mathbf{p}}(\xi^{\frac{1}{2}} m_1)\right]^{-1} \\
\text{Vertex1:}(p' \to 0) & \mathcal{A}'_5 g_{\lambda\rho} \\
\text{Propagator2:}(p' \to 0) & 1/m_H^2 \\
\text{Vertex2:}(p' \to 0) & \mathcal{A}_5 g_{\mu\nu} .
\end{array}
$$

The polarisation response functions are given by

$$
\pi^J = -\frac{\mathcal{A}_5 \mathcal{A}'_5}{m_H^2}\left\{3Y_g^J[m_1, \mu_1] + \xi Y_g^J[\xi^{\frac{1}{2}} m_1, \mu_1]\right\} . \tag{B16}
$$

Manuscript received 20 December 1994, accepted 21 February 1995